Verification

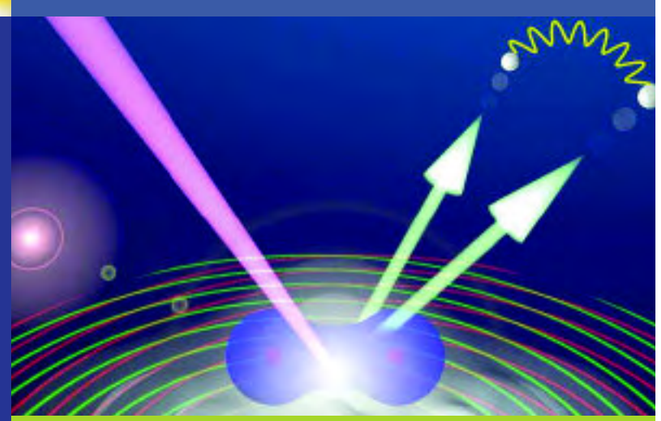

Demand

Scientific **HIGHLIGHTS** 06/7

Low-energy Acoustic Plasmons at Metal Surfaces

B. Diaconescu[1], K. Pohl[1], L. Vattuone[2], L. Savio[2], Ph. Hofmann[3], V.M. Silkin[4], J.M. Pitarke[5], E.V. Chulkov[4], P.M. Echenique[4], D. Farías[6], and M. Rocca[7]

Here we show that, in contrast to the well-established belief, a low-energy collective excitation mode can be found on bare metal surfaces. This mode has an acoustic-like dispersion and was observed on Be(0001) using angle-resolved electron energy loss spectroscopy. First-principles calculations show that it is caused by the coexistence of a partially occupied quasi 2D surface-state band with the underlying 3D bulk electron continuum and that the non-local character of the dielectric function prevents it from being screened out by the 3D states.

Nearly two-dimensional (2D) metallic systems permit the existence of low-energy collective excitations, so-called 2D plasmons, which are not found in a three-dimensional metal. These excitations have caused considerable interest because their low energy allows them to participate in many dynamical processes involving electrons and phonons. Metals often support electronic states that are confined to the surface forming a nearly 2D electron density layer. However, it was argued that these systems could not support low-energy collective excitations because these would be screened out by the underlying bulk electrons. Here we show that, in contrast to expectations, a low-energy collective excitation mode can be found on bare metal surfaces[1].

The experiment was performed in an ultrahigh vacuum apparatus equipped with an angle-resolved high resolution electron energy loss (EEL) spectrometer for Be(0001) at room temperature. Figure 1 shows typical angle-resolved EEL spectra taken along the ΓM direction for positive values of the momentum transfer q_{II}. A broad peak is observed to disperse as a function of q_{II} and the energy of this mode is found to approach zero linearly for vanishing q_{II} values. Our experimental data clearly show the acoustic-like character of this excitation within the limits of the experimental errors.

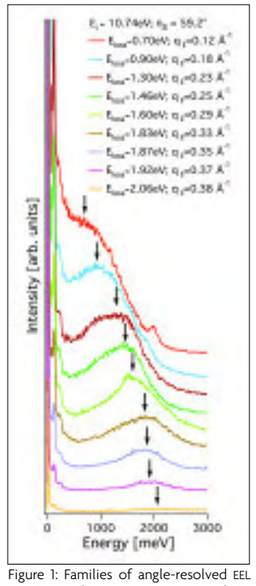

Figure 1: Families of angle-resolved EEL spectra. Each spectrum corresponds to a different electron momentum transfer component parallel to the surface q_{II}.

1 Department of Physics and Material Science Program, University of New Hampshire, Durham, USA **2** CNISM and Dipartimento di Fisica, Università di Genova, Italy **3** Institute for Storage Ring Facilities and Interdisciplinary Nanoscience Center (iNANO), University of Aarhus, Denmark **4** Donostia International Physics Center, Centro de Fisica de Materiales-CSIC, UPV/EHU, San Sebastián, Spain **5** CIC nanoGUNE Consolider and Materia Kondentsatuaren Fisika Saila, UPV/EHU, San Sebastián, Spain **6** Departamento de Fisica de la Materia Condensada, Universidad Autónoma de Madrid, Spain **7** IMEM-CNR and Dipartimento di Fisica, Università di Genova, Italy

Published in **Nature**

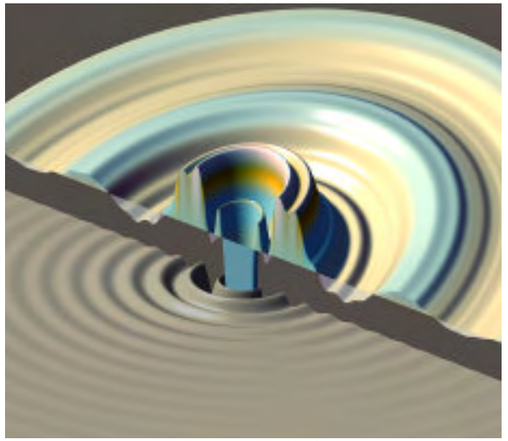

Figure 2: Charge density oscillations at the metal surface corresponding to acoustic surface plasmon (top) in comparison with conventional Friedel oscillations (bottom).

This new mode allows confinement of light on nanometric surfaces in a broad frequency range.

Many metal surfaces such as Be(0001) and the (111) surfaces of noble metals support a partially occupied band of Shockley surface states with energies near the Fermi level. Here we show that the experimental data can be interpreted as a novel collective electronic excitation, acoustic surface plasmon (ASP), of the quasi-2D surface charge distribution if a full non-local dynamical screening at the surface is considered. Information on collective electronic excitations at surfaces is obtained from the peak position of the imaginary part of the surface response function which depends on q_{II} and frequency. We calculate first the single particle energies and wave functions which describe the surface band structure. With these wave functions and energies we then compute the surface response function. We are able to reproduce the experimental dispersion quantitatively by employing an *ab-initio* description of the surface electronic structure which greatly increases our confidence in the interpretation of the experiment.

ASP results from the interplay of the partially occupied electronic surface state, acting as a 2D electron density overlapping in the same region of space with the bulk electron gas, and the long-range Coulomb interaction manifested in the form of 3D dynamical screening of the 2D surface electron density. It corresponds to the out-of-phase charge oscillations between 2D and 3D subsystems at the metal surface and its dispersion is mainly determined by the surface-state Fermi velocity v_F. Figure 2 shows these oscillations in comparison with conventional Friedel charge oscillations. ASPs, as reported here, owe their existence to the non-local screening due to bulk electrons at surfaces characterized by a partially occupied surface-state band lying in a wide bulk energy gap and as such they should be a common phenomenon on many metal surfaces. Moreover, due to the acoustic-like dispersion, it will affect the electron dynamics near the Fermi level much more dramatically than regular 2D plasmons. The possibility to excite this collective mode at very low energies can therefore lead to new situations at metal surfaces due to the competition between the incoherent electron-hole excitations and the new collective coherent mode. Many phenomena, such as electron, phonon and adsorbate dynamics as well as chemical reactions with characteristic energies lower than few eV can be significantly influenced by the opening of a new low-energy decay channel such as ASP. Of particular interest is the interaction of the ASP with light as this new mode can serve as a tool to confine light on surface areas of a few nanometers in a broad frequency range up to optical frequencies.

[1] B. Diaconescu, K. Pohl, L. Vattuone, L. Savio, Ph. Hofmann, V.M. Silkin, J.M. Pitarke, E.V. Chulkov, P.M. Echenique, D. Farías and M. Rocca, Nature **448**, 57 (2007).

Attosecond Spectroscopy in Condensed Matter

A.L. Cavalieri[1], N. Müller[2], Th. Uphues[1,2], V.S. Yakolev[3], A. Baltuska[4], B. Horvath[1], B. Schmidt[5], L. Blümel[5], R. Holzwarth[5], S. Hendel[2], M. Drescher[6], U. Kleineberg[3], P.M. Echenique[7], R. Kienberger[1], F. Krausz[1,3], and U. Heinzmann[2]

Electrons require tens to hundreds of attoseconds (1 as = 1 quadrillionth second = 0.000 000 000 000 000 001 second) to travel between neighbouring atoms in solids. While astonishingly brief, these attosecond travel times will ultimately limit the speed of electronics in the future. Advancing technology toward this ultimate limit will rely on the capability of real-time measurement and finally, control of electron transport in solids with attosecond resolution. Recently, in the Laboratory of Attosecond and High-Field Physics at the Max-Planck-Institute of Quantum Optics, Adrian Cavalieri and his collaborators from Bielefeld, Hamburg, Vienna and San Sebastian achieved the first of these goals by measuring the difference between the travel times of two different types of electrons through several atomic layers. The experiment constitutes the first attosecond-scale measurement in condensed matter and opens the door to control of electron transport in solids on the atomic scale.

The controlled transport of electric charge by electrons through nano-scale electric circuits forms the basis of modern electronics, used, for example, in computers, communication devices and measuring instruments. In state-of-the-art electronic circuits, electrons are driven by a microwave voltage, which is capable of switching on and off current within a fraction of a nanosecond (1 ns = 1 billionth second = 0.000 000 001 second). The switching time determines the number of calculations that can be performed by a computer clocked by this chip during a certain period of time. Ultimately, the rapidity of switching is limited by the time it takes for the electrons to travel through the structures used for guiding and controlling their current. Smaller structures lead to faster switching speeds and a higher density of information flow. The quest for ever smaller nano-structures in solid-state electronics and for atomic assemblies in molecular electronics is driven by these simple relationships. The distance between neighboring atoms in a crystal lattice or in a molecule constitutes the smallest possible length scale for channelling and switching current for the purpose of information processing. The time it takes for electrons travelling distances on the atomic scale is naturally clocked in attoseconds, implying the feasibility of switching electric current more than a trillion times in atomic-scale (solid-state or molecular) circuitry. This would result in the emergence of Petahertz electronics, in which the direction of electric current can be changed at a rate of several trillion times per second, some hundred thousand times higher than permitted by present-day electronics.

Measuring solid-state electronic processes at the theoretical ultimate speed for electronics.

1 Max-Planck-Institut für Quantenoptik, Garching, Germany **2** Fakultät für Physik, Universität Bielefeld, Germany **3** Department für Physik, Ludwig-Maximilians-Universität, Garching, Germany **4** Institut für Photonik, Technische Universität Wien, Austria **5** Menlo Systems GmbH, Martinsried, Germany **6** Institut für Experimentalphysik, Universität Hamburg, Germany **7** Centro de Física de Materiales-CSIC, UPV/EHU and Donostia International Physics Center, San Sebastián, Spain

Published in **Nature**

A first essential step on the long way towards ultimate-speed electronics, limited only by the time required for an electron to travel between neighbouring atoms, is the development of techniques to capture electronic charge transport in atomic-scale structures on the attosecond time scale. This first step was recently successfully demonstrated in a proof-of-principle experiment at the Max Planck Institute of Quantum Optics (MPQ) in Garching, Germany, in which researchers observed attosecond electric charge transport across several atomic layers near the surface of a crystalline solid in real time[1].

The MPQ team, along with collaborators from the University of Bielefeld, shone a 300-attosecond pulse of extreme ultraviolet (XUV) light along with an infrared laser pulse comprising a few, well-controlled oscillation cycles of its electric field on the surface of a tungsten crystal. The attosecond pulse penetrates the tungsten crystal, and XUV photons are absorbed, which results in freeing both loosely-bound electrons, responsible for conduction, and electrons bound tighly to the cores of the atoms forming the crystal lattice. These electrons are excited simultaneously and speed from a depth of several atomic layers, to the surface, at a different speed: the loosely-bound (conduction) electrons travel faster than the tightly-bound (core) electrons. Once at the surface, the electron's initial velocity, which depends on the XUV photon energy and the electron's original binding energy (as predicted by Einstein more than a century ago), is changed by the laser electric field, E(t), and this change can be detected by a time-of-flight detector. By changing the electrons' velocity in a controlled fashion, the rapidly oscillating laser field serves as a stopwatch with attosecond resolution. By careful examination of the measured data, the researchers were able to determine that the loosely-bound conduction electrons were emitted approximately 100 attoseconds earlier than their tightly-bound counterparts. This delay indicates that, inside the tungsten crystal, the freed conduction electrons travel twice as fast as those liberated from states localized near the atomic cores.

This work demonstrates the technical capability of measuring electronic charge transport across atomic layers in real time with attosecond temporal resolution. Future measurements of this type will allow for research into structures and technologies for speeding up state-of-the-art electronics by several orders of magnitude.

Probing travel between neighboring atoms in a solid at an attosecond pace.

[1] A.L. Cavalieri *et al.*, Nature **449**, 1029 (2007).

The Simplest Double Slit: Interference and Entanglement in Double Photoionization of H_2

D. Akoury[1,2], K. Kreidi[1], T. Jahnke[1], Th. Weber[1,2], A. Staudte[1], M. Schöffler[1], N. Neumann[1], J. Titze[1], L.Ph.H. Schmidt[1], A. Czasch[1], O. Jagutzki[1], R.A. Costa Fraga[1], R.E. Grisenti[1], R. Díez Muiño[3], N.A. Cherepkov[4], S.K. Semenov[4], P. Ranitovic[5], C.L. Cocke[5], T. Osipov[2], H. Adaniya[2], J.C. Thompson[6], M.H. Prior[2], A. Belkacem[2], A.L. Landers[6], H. Schmidt-Böcking[1], and R. Dörner[1]

The wave nature of particles is rarely observed, in part because of their very short de Broglie wavelengths in most situations. However, even with wavelengths close to the size of their surroundings, the particles couple to their environment, and the resulting decoherence is thought to be a main cause of the transition from quantum to classical behavior. How much interaction is needed to induce this transition? Our work shows that a photoelectron and two protons form a minimum particle/slit system and that a single additional electron constitutes a minimum environment.

One of the most powerful paradigms in the exploration of quantum mechanics is the double-slit experiment. Thomas Young was the first to perform such an experiment, as early as 1801, with light. It took until the late 1950s, long after the experimental proof of the wave nature of particles was revealed, for a similar experiment to be carried out with electrons. A decade later, Cohen and Fano suggested that a homonuclear molecule could be used as the slit-scattering center: Because of the coherence in the initial molecular state, the absorption of one photon by the homonuclear molecule launches two coherent electron waves at each of the protons of the molecule.

In Ref. [1], we extend this idea to the case of double photoionization (i.e., two electrons are emitted as a consequence of the absorption of a single photon), and show that the interference pattern of these waves is clearly visible in the angular distribution of the electrons, with respect to the molecular axis. Furthermore, interference fringes observed in the angular distribution of a single electron are lost through its Coulomb interaction with the second electron, though the correlated momenta of the entangled electron pair continue to exhibit quantum interference.

Experiments were performed at the Advanced Light Source, of the Lawrence Berkeley National Laboratory. The orientation of the H_2 molecule, or molecular double slit, was measured for each fragmentation by detecting the emission direction of the two protons. Once the two electrons are ejected, the protons rapidly fly apart along the molecular axis, driven by their mutual Coulomb repulsion. A multiparticle imaging technique was used to detect all particles. Theoretical calculations nicely reproduce the measured angular distributions of the emitted electrons and serve to explain the loss of coherence when the sharing of kinetic energy between the two electrons is varied.

1 Institut für Kernphysik, Universität Frankfurt, Germany **2** Lawrence Berkeley National Laboratory, CA, USA **3** Donostia International Physics Center and Centro de Física de Materiales CSIC-UPV/EHU, San Sebastián, Spain **4** State University of Aerospace Instrumentation, St. Petersburg, Russia **5** Department of Physics, Kansas State University, USA **6** Department of Physics, Auburn University, AL, USA

Published in **Science**

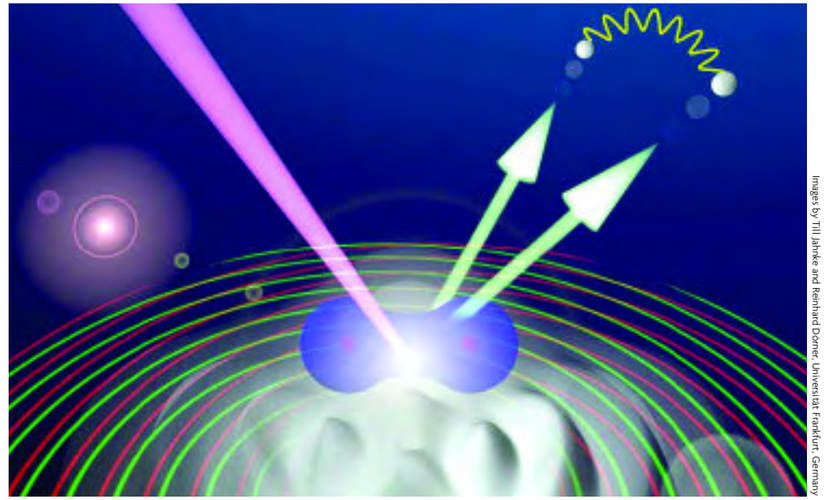

Images by Till Jahnke and Reinhard Dörner, Universität Frankfurt, Germany

The particle-wave duality put to the test at a scale smaller than ever before.

It is instructive to think of the electronic two body system as split into its subsystems and to consider one subsystem as the environment of the other. The strong Coulomb interaction entangles the two subsystems and leads to a position-dependent modification of phase of the single-particle wave function inside each of the two subsystems. The entanglement of the electrons in the pair is directly visible in their mutual angular distribution and is further evidenced by the observation that selecting the momentum of one electron makes the interference pattern of its partner reappear.

This work thus reveals that a very small number of particles suffices to induce the emergence of classical properties, such as the loss of coherence. A four-body system, such as fragmented molecular hydrogen, acts as a double slit in the sense that coherence is lost in a subsystem of entangled electrons. Such a fundamental system facilitates the study of the influence of interelectronic Coulomb interactions on the coherence properties of a single electron. In solid-state-based quantum computing devices, the understanding and control of such electron-electron interaction represents one of the key challenges.

[1] D. Akoury *et al.*, Science **318**, 949 (2007).

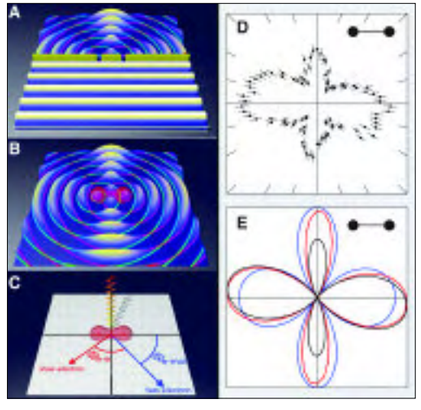

A photoelectron and two protons form a minimum particle/slit system; a single additional electron constitutes a minimum environment.

Role of Spin-Orbit Coupling and Hybridization Effects in Electronic Structure of Ultrathin Bi Films

T. Hirahara[1], T. Nagao[2], I. Matsuda[1], G. Bihlmayer[3], E.V. Chulkov[4,5], Yu.M. Koroteev[4,6], P.M. Echenique[4,5], M. Saito[7], and S. Hasegawa[1]

Electronic structure of Bi(001) ultrathin films (thickness ≥ 7 bilayers) on Si(111)-7x7 was studied by angle-resolved photoemission and first-principles calculations. In contrast to the semimetallic nature of bulk Bi, both the experiment and theory demonstrate the metallic character of the films with the Fermi surface formed by spin-orbit-split surface states showing little thickness dependence. Below the Fermi level we clearly detect quantum well states (QWS) at the M point which were surprisingly found to be non-spin-orbit split.

Semimetal bismuth is one of the most extensively studied elements in solid state physics because of its extreme physical properties. For example, it is the most diamagnetic and has the highest Hall coefficient, while it shows very high resistivity and the lowest heat conductivity of all metals. Bi has tiny hole and electron pockets at the T and L points, respectively (Figure 1(d)), and therefore it has a very large Fermi wavelength, λ_F, of about 30 nm. Because of this large λ_F, nanosized objects of Bi in the range of several tens of nanometers have been towards the development of quantum-size-effect-based devices. It was predicted that with the film thickness the lowest quantized subband of the electron pocket is raised to an energy higher than the highest hole subband, a band gap will develop semimetal-to-semiconductor (SMSC) transition at ≈30 ~nm.

Such picture is based on the bulk band structure, but when the system downsizes to nanometer scale, significant contribution from the surface effects will make the system even more intriguing.

In the present letter, we report on the angle-resolved photoemission (ARPES) study of ultrathin films of Bi(001) with thicknesses up to a few nanometers (d«λ_F). In remarkable contrast to the predicted SMSC transition, we find that the films are highly metallic and their Fermi surface formed by SO-split surface states has little thickness dependence. On the other hand, the number of states rapidly increases with the film thickness at M below E_F, which can be clearly identified as quantum well states (QWS). Our relativistic first-principles calculation shows that these QWS s are spin-degenerate in striking contrast to the strong SO-split surface state bands[1,2]. This suggests that in spite of the obvious structural inequality of the top and the bottom interfaces, the electronic structure of the film behaves as if it preserves space-inversion symmetry, indicating weak substrate-film interaction. We further clarify that the hybridization of the QWSs with the SSs makes the SS bands QWS-like near the M point and lose their spin-orbit property. Our ARPES experiments were performed in UHV with a commercial electron spectrometer (Gammadata Scienta SES-100) using unpolarized HeI (21.2~eV) radiation at 130~K. The calculations have been done using the full-potential linearized augmented plane wave method in film geometry as implemented in the FLEUR program.

1 Department of Physics, School of Science, University of Tokyo, Japan **2** Nanomaterials Lab, National Institute for Materials Science, Ibaraki, Japan **3** IFF-FZ, Forschungszentrum Jülich, Germany **4** Donostia International Physics Center, San Sebastián, Spain **5** Centro de Física de Materiales CSIC, UPV/EHU, San Sebastián, Spain **6** Institute of Strength Physics and Materials Science, Russian Academy of Sciences, Tomsk, Russia **7** Graduate School of Natural Science and Technology, Kanazawa University, Kakuma, Kanazawa, Japan

Published in **PRL**

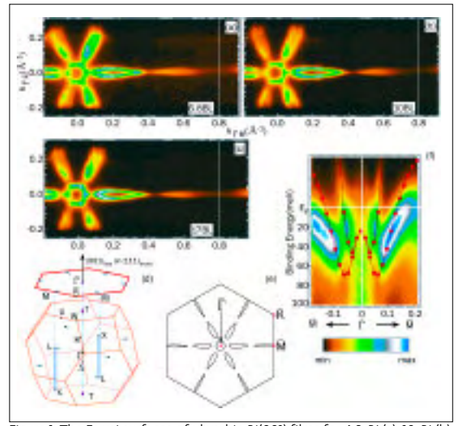

Figure 1: The Fermi surfaces of ultrathin Bi(001) films for 6.8-BL(a), 10-BL(b), and 17-BL(c) films.

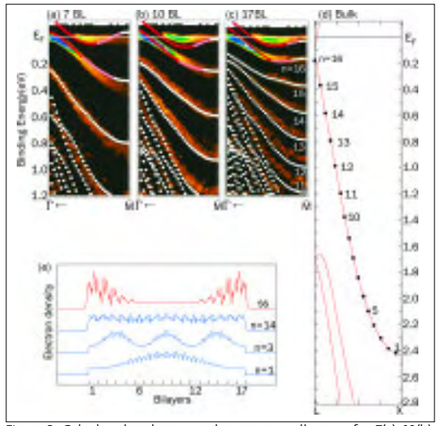

Figure 2: Calculated and measured quantum-well states for 7(a), 10(b) and 17(c) bilayer Bi(001) films along the ΓM direction for k › 0.3 ≈$^{-1}$.

Figure 1 shows the photoemission intensity distribution at the Fermi level for 6.8, 10, and 17~BL Bi(001) films respectively. The intensity increases linearly from black (minimum) to dark blue (maximum). In panel (e) we show the schematic drawing of the Fermi surface of the ultrathin films. There is a hexagonal electron pocket around the Γ point and six hole lobes along the ΓM direction. It is evident that these features are completely different from the projected bulk Fermi surface shown in panel (d) and show strong metallicity, contrary to the prediction of SMSC transition. Also, they have hardly any thickness dependence and possess sixfold symmetry. This means that they are formed by surface states having strong two-dimensional character[1].

Figure 2 shows the calculated results together with the measured band dispersion for 7 (6.8 for the experiment), 10, and 17 BL films, respectively, near the M point. For the two uppermost states close to E_F, the region where the electron density is localized in the surface is represented in red, and states localized weaker in the surface are indicated in pink. The rest of the states are shown in white. It is clear that the calculation is consistent with the overall experimental band dispersion reflecting the symmetry of the whole film. The states located at M are particularly well reproduced. Unexpectedly, this shows that electrons in our ultrathin films really behave as if the space-inversion symmetry is preserved even though that the two interfaces are asymmetric as one side is vacuum and the other side is silicon.

In conclusion, our ARPES measurements and calculations of ultrathin Bi(001) films showed that the films are highly metallic in contrast to the scenario of SMSC transition. They have Fermi surfaces with little thickness dependence formed by SO-split surface states. Below the Fermi level, QWSs have been observed for the first time in Bi films. These QWSs are spin-degenerate because of the weak substrate-film interaction as well as their small surface charge density which make these states insensitive to the surface structural asymmetry. When the surface state hybridizes with the degenerate QWSs near the M point, they undergo qualitative changes from the SS character to the QWS one.

[1] Y.M. Koroteev, G. Bihlmayer, J.E. Gayone, E.V. Chulkov, S. Blügel, P.M. Echenique, and Ph. Hofmann, Phys. Rev. Lett. **93**, 046403 (2004).
[2] T. Hirahara, T. Nagao, I. Matsuda, G. Bihlmayer, E.V. Chulkov, Yu.M. Koroteev, P.M. Echenique, M. Saito, and S. Hasegawa, Phys. Rev. Lett. **93**, 196802 (2004).

In remarkable contrast to the predicted SMSC transition, the Bi films are found to be highly metallic.

Polymer Chain Dynamics in a Random Environment: Heterogeneous Mobilities

K. Niedzwiedz[1], A. Wischnewski[1], M. Monkenbusch[1], D. Richter[1], A.-C. Genix[2], A. Arbe[3], J. Colmenero[2,3,4], M. Strauch[5], and E. Straube[5]

We present a neutron scattering study on a miscible blend of two polymers with greatly different glass transition temperatures T_g. Under such conditions, the nearly frozen high-T_g component imposes a random environment on the mobile chain. The results demand the consideration of a distribution of heterogeneous mobilities and demonstrate that the larger scale dynamics of the fast component is not determined by the average local environment alone. This distribution of mobilities can be mapped quantitatively on the spectrum of local relaxation rates measured at high momentum transfers.

The investigation of dynamic miscibility in polymer blends, i.e. the question how friction arises in chemically heterogeneous systems at present is a very active area of research[1]. At temperatures well above the component glass-transition temperatures T_g, the concept of segment self-concentration[2] provides a rather successful description of the component dynamics of a large number of polymer blends[1]. Due to chain connectivity, this self-concentration is always enhanced locally and determines the component dynamical behavior. On the other hand, in systems with greatly different component T_g's a decoupling of the dynamics of both components has been reported [poly(ethylene oxide)/poly(methyl methacrylate) (PEO/PMMA), polystyrene/poly(vinyl methyl ether) and PEO/poly(vinyl acetate)][2]. For example, in the system PEO/PMMA [T_g(PEO)≈200K, T_g(PMMA)≈400K], an enormous dynamic asymmetry (up to 12 orders of magnitude different local relaxation times) has been reported from NMR studies. Under such conditions, the low-T_g component moves in the random environment created by the frozen high-T_g component. Beyond its interest for blend dynamics including plasticizing effects, this situation may create an experimental testbed facilitating investigations of polymer chains in random environments, which presently was mainly studied theoretically (see, e.g. [3] and references therein).

Dynamically asymmetric polymer blends constitute an experimental testbed facilitating investigations of polymer chains in random environments.

1 Institut für Festkörperforschung, Forschungszentrum Jülich, Germany **2** Donostia International Physics Center, San Sebastian, Spain **3** Centro de Física de Materiales-CSIC, UPV/EHU, San Sebastian, Spain **4** Departamento de Física de Materiales, UPV/EHU, San Sebastian, Spain **5** Fachbereich Physik, Martin-Luther Universität Halle-Wittenberg, Halle, Germany

Published in **PRL**

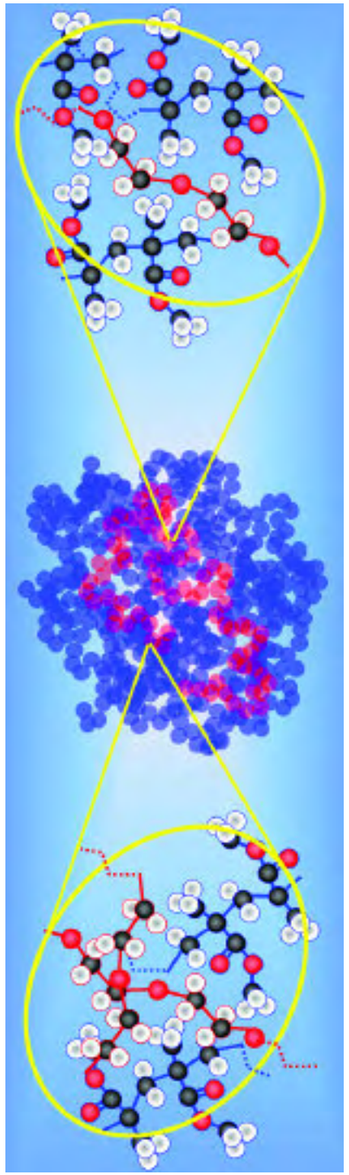

Representation of a PEO/PMMA blend: in the middle, a PEO chain (red) is immersed in a sea of PMMA chains (blue) (large scales). In the atomistic views (local scales, top and bottom), different local environments are illustrated [carbons in black, oxygens in red and hydrogens in white; the colour of the bonds indicates whether the atom belongs to PEO (red) or to PMMA (blue)].

This study[4] is devoted to the space-time evolution of the PEO dynamics in PMMA at different scales using quasielastic neutron scattering. Exploiting the selectivity offered by this technique combined with isotopic substitution, we isolate the self and the collective (single chain dynamic structure factor) dynamics of the PEO component in the blend. With incoherent scattering we have followed the hydrogen self-motions of PEO in a time window up to about 1ns and displacements up to 1nm. This local dynamics is found to be fast. On the other hand, the collective chain dynamics has been followed up to about 80ns by coherent scattering. These motions are apparently more than an order of magnitude slower than the timescales obtained by incoherent scattering. This is in clear contradiction to the expectation from standard theories for chain dynamics in a polymer melt (Rouse motion, see, e.g.[5]). Thus, a clear decoupling of self- and collective motions arises in such a situation of strong dynamic asymmetry at intermediate length scales.

Assuming a rather flat energy landscape but with locally varying mobility of the components, we introduce a distribution of friction coefficients and implement them in a Rouse model with random friction. In this way can quantitatively and consistently describe the local, the intermediate as well as the more global dynamics, since the distribution invoked is the same for all length scales considered (≈Å to several nm). The analysis shows that the chain dynamics in a random environment may be characterized by a set of random friction coefficients causing a successive slowing down of motion depending on the observed scale.

[1] T.P. Lodge and T.C.B. McLeish, Macromolecules **33**, 5278 (2000).
[2] J. Colmenero and A. Arbe, Soft Matter **3**, 1474 (2007).
[3] G. Migliorini, V.G. Rostiasvili and T.A. Vilgis, Eur. Phys. J. B **33**, 61 (2003).
[4] K. Niedzwiedz, A. Wischnewski, M. Monkenbusch, D. Richter, A.-C. Genix, A. Arbe, J. Colmenero, M. Strauch and E. Straube, Phys. Rev. Lett. **98**, 168301 (2007).
[5] D. Richter, M. Monkenbusch, A. Arbe and J. Colmenero, Advances in Polymer Science, Vol. **174** (2005).

The distribution of mobilities can be mapped quantitatively on the spectrum of local relaxation rates.

Extreme Ultrafast Dynamics of Quasiparticles Excited in Surface Electronic Bands

P. Lazić[1,2], V.M. Silkin[1], E.V. Chulkov[1,3], P.M. Echenique[1,3], B. Gumhalter[1,4]

We develop a many-body description of non-adiabatic dynamics of quasi-particles in surface bands valid on the extreme ultra-short time scale by combining the formalism for calculation of quasi-particle survival probabilities with the self-consistent treatment of electronic response of the system. Applying this approach to the Cu(111) surface we assess the behavior and intervals of pre-asymptotic electron and hole dynamics in surface bands and locate the transition to asymptotic regime of exponential quasi-particle decay characterized by the Fermi golden rule-type of transition rate.

The development of time resolved electron spectroscopies has enabled measurements of the surface electronic processes in the real time. Such experiments provide direct insight in temporal evolution of the studied systems from which information on the various relaxation processes that govern the dynamics of excited quasiparticles can be deduced. Descriptions of these processes are commonly given in terms of the rate constants that characterize asymptotic relaxation of quasiparticle states. However, if the act of measurement proceeds on the time scale comparable to or shorter than that of relaxation and de-coherence processes the thus probed quasiparticle evolution may considerably differ from asymptotic behavior described by the rate constants. In this context it is of particular interest to pinpoint the intervals in which descriptions of ultrafast quasiparticle dynamics in terms of few rate constants cease to be valid.

Here we develop the first non-asymptotic many-body description of propagation of electrons (holes) after their promotion into surface states[1]. To assess ultrafast dynamics of promoted quasiparticles we calculate the survival probability that describes quasiparticle evolution upon its injection into a 2D momentum eigenstate within the n-th surface band in which its subsequent motion is affected by dynamic interactions with the substrate. These interactions give rise to intra- and inter-band transitions of the quasiparticle in which the energy ω and 2D momentum Q are exchanged with the substrate excitations. We illustrate different stages of ultrafast quasiparticle dynamics in surface bands for the benchmark surface Cu(111) with one electron introduced in the image potential (IS) band or one hole created in the surface state (SS) band. We start from the self-consistent RPA response function calculated for a N-layer slab (N=31) that models the Cu(111) surface by using the effective potential. This model enables a systematic treatment of intra- and inter-band transitions on equivalent footing. The oscillator strengths were calculated using linear combinations of pairs of symmetric and anti-symmetric electron wavefunctions from the same slab calculation. From this we computed the excitation spectrum on a (Q,ω) grid for combinations of indices $(0 \le n,n' \le n_{max})$ that cover the relevant intra- and inter-band transitions.

1 Donostia International Physics Center, San Sebastián, Spain **2** Rudjer Boskovic Institute, Zagreb, Croatia **3** Centro de Física de Materiales-CSIC, Facultad de Ciencias Químicas, UPV/EHU, San Sebastián, Spain **4** Institute of Physics, Zagreb, Croatia

Published in **PRL**

Figure 1 shows the computed intensity of the IS-projected intra-band component (n'=n=IS) of the excitation spectrum $S_{n',n}(Q,\omega)$ over the phase space of excitation energies ω and wavevectors Q relevant in the calculations of survival probability $L_{K,n}(t)$. Dominant contributions to the intensity come from the surface plasmon which disperses along a parabolic curve starting at the point Q=0 and ω =7.6 eV, the bulk plasmon whose dispersion curve starts at ω =12.6 eV, and the electron-hole (e-h) quasi-continuum with maximum intensity in the region encompassed by the parabolas $\omega = Q^2/2m_n \pm Qv_{F,n}$ and $0 \le \omega \le Qv_{F,n} - Q^2/2m_n$ ($v_{F,n}$ is the Fermi velocity in the n-th band). Qualitatively similar behavior of $S_{n',n}(Q,\omega)$ is obtained for other combinations of indices n and n'.

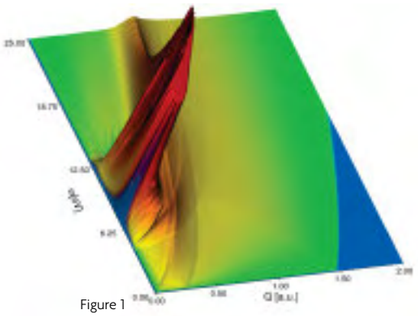

Figure 1

Different stages of ultrafast quasiparticle dynamics are analysed.

Temporal behavior of the survival probability $L_{K,n}(t)$ can be calculated for initial values of n and K using the above obtained results. Figure 2 shows $L_{K,IS}(t)$ for an electron created in the IS-band on Cu(111) surface with initial wavevectors K=0.01 and K=0.05 a.u. The very early Gaussian decay is superseded by a superposition of oscillations arising from non-adiabatic (off-resonant) excitations of surface plasmons in the slab and a gradual build up of the $w_{K,n}$-corrected Fermi's golden rule (FGR) decay arising from resonant excitation of e-h pairs. Due to the off-the energy-shell character of plasmon excitations their amplitude diminishes as $t \to \infty$. We find that for K=0.01 inter-band $IS \to SS$ transitions contribute about 39% to the total decay rate $\Gamma_{K,IS}$, and the remaining 61% arise from inter-band transitions into bulk bands, in agreement with earlier calculations.

Figure 2 enables the identification of three distinct regimes of ultrafast quasiparticle dynamics. The early Zeno regime ($0 < t < 1$ *fs*) is followed by pre-asymptotic non-Markovian evolution with superimposed off-resonant excitation of surface plasmons and resonant excitation of e-h pairs. This structure persists up to t~10 fs, and only past that time do the off-resonant plasmon excitations die out, and the steady state asymptotic evolution governed by the corrected FGR decay takes over. However, even long past that time, the bare FGR decay $\exp(-\Gamma_{K,n}t)$ is not yet approached, signifying that extreme ultrafast dynamics of quasiparticles promoted in surface bands requires pre-asymptotic description of relaxation and decay processes.

[1] P. Lazić, V.M. Silkin, E.V. Chulkov, P.M. Echenique and B. Gumhalter, Physical Review Letters 97, 086801 (2006).

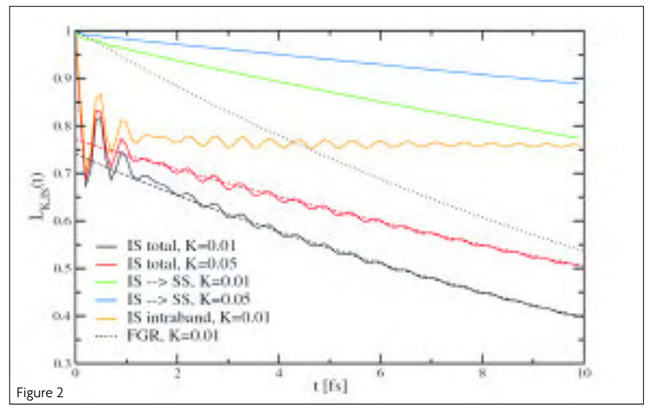

Figure 2

Published in **Macromol**

Unravelling Structure and Dynamics of PMMA by Combining Neutron Scattering and MD-Simulations

A.-C. Genix[1], A. Arbe[2], F. Alvarez[3], J. Colmenero[1,2,3], W. Schweika[4], B. Farago[5], A. Wischnewski[4], and D. Richter[4]

In this work we have demonstrated the power of the combination of neutron scattering techniques and fully atomistic MD-simulations to gain deep insight into the structural and dynamical features of polymers at intra- and intermolecular levels.

Poly(methyl methacrylate) (PMMA) is an interesting glass-forming polymer since it is the 'small baby' of the family of poly (n-alkyl methacrylates) (PnMAs). The high-order members of this series show intriguing features as nanophase separation and two different glass-transitions[1]. In this work[2,3], we have combined neutron scattering and fully atomistic molecular dynamics simulations to investigate the short-range order and dynamics at local length scales of syndiotactic PMMA.

We start with the structural study[2]. Selectively deuterating parts of the PMMA monomer we have accessed five different partial structure factors in the glassy state by neutrons, and polarization analysis has allowed isolating the coherent contribution to the total scattering. The different measured partial structure factors show qualitatively different features with respect to peak positions and heights and provide a very critical check to validate the simulated structure. In order to gain deep insight on the structure, we have grouped the simulations results in terms of three molecular sub-structures: the main chain, the α-methyl group and the ester-side group (see Figure). The study of the resulting partial structure functions has revealed the origin of the diffraction peaks, including those in the X-rays pattern reported in the literature. In addition, a real-space evaluation of the characteristic radial distribution functions has allowed separating intra- and interchain contributions to the total correlation functions. We have found that (i) PMMA exhibits a strong local order with an average main-chain distance of ≈ 8.6 Å; (ii) this is the only average interchain distance and thus no precursor effect of a layered structure is found; (iii) the main chain shows a persisting all-trans structure; (iv) a strong anti-correlation between the main chain and the ester-side groups, together with an interdigitation of the side groups, suggest a marked separation between the backbone and the side-group spatial arrangements. The deduced structure is depicted in the Figure. It could be interpreted as a precursor effect of the suggested nano-phase separation in higher order PnMA's.

Only the combination of both techniques can provide such reliable insight into the short-range order structure and dynamics of polymer melts.

1 Donostia International Physics Center, San Sebastian, Spain **2** Centro de Física de Materiales-CSIC, UPV/EHU, San Sebastian, Spain **3** Departamento de Física de Materiales, UPV/EHU, San Sebastian, Spain **4** Institut für Festkörperforschung, Forschungszentrum Jülich, Germany **5** Institut Laue-Langevin, Grenoble, France

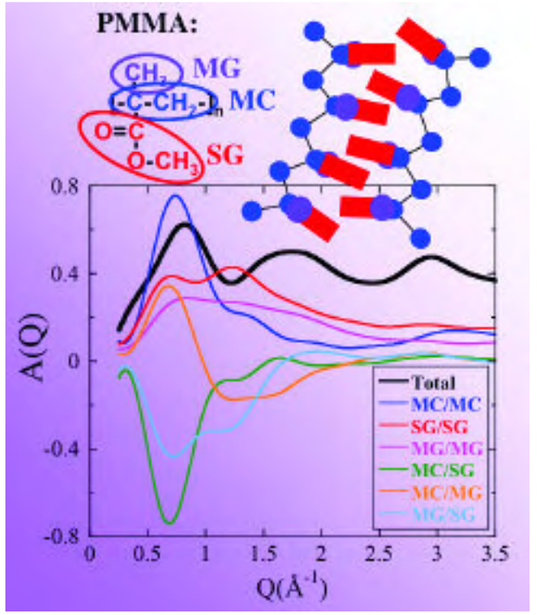

Fourier transform of the different partial radial distribution functions corresponding to the different atomic correlations within the molecular groups considered (see monomer scheme). The image illustrates the suggested interdigitation of the side groups.

The separation between the backbone and the side-group spatial arrangements could be interpreted as a precursor effect of the suggested nano-phase separation in higher order PnMA's.

Moving to the dynamics study above the glass-transition temperature[3], the incoherent scattering measured by backscattering on a sample with deuterated ester-methyl groups has revealed the single-particle motions of hydrogens in the main-chain and in the α-methyl groups. Moreover, with neutron spin echo experiments on the fully deuterated sample we have accessed the collective motions at the two first maxima of the structure factor. The simulated cell shows a dynamical behavior that, allowing a shift in temperature, reproduces very accurately all the experimental results. The combined analysis of both sets of data has shown that: (i) the segmental relaxation involving backbone atoms deviates from Gaussian behavior; (ii) the dynamics is extremely heterogeneous: in addition to the subdiffusion associated to the α-process and the methyl-group rotations, we have found indications of a rotational motion of the ester-side group around the main chain; (iii) at a given momentum transfer and depending on the molecular groups considered, the timescales for collective motion are spread over about one order of magnitude, the correlations involving the main chain decaying much more slowly than those relating side groups; (iv) at the length scale characteristic for the overall periodicity of the system (that corresponding to the first structure factor peak), the experimentally observed collective dynamics strongly relates to the backbone motions and is of interchain character; there, coherency effects are observed for all correlations, though side groups display weaker collectivity; (v) at the second structure factor peak, coherency remains only for correlations involving the main-chains.

[1] M. Beiner, Macromol. Rapid Commun. **22**, 869 (2001).
[2] A.-C. Genix, A. Arbe, F. Alvarez, J. Colmenero, W. Schweika, and D. Richter, Macromolecules **39**, 3947 (2006).
[3] A.-C. Genix, A. Arbe, F. Alvarez, J. Colmenero, B. Farago, A. Wischnewski, and D. Richter, Macromolecules **39**, 6260 (2006).

Why N_2 Molecules with Thermal Energy Abundantly Dissociate on W(100) and Not on W(110)?

M. Alducin[1], R. Díez Muiño[1,2], H.F. Busnengo[3], and A. Salin[1]

Dissociation of N_2 on tungsten is considered as an emblematic example on how chemical reactivity can dramatically depend on the crystal surface structure. Low energy N_2 molecules easily dissociate on W(100) but not on W(110). This remarkable difference in reactivity has been conventionally attributed to the respective non-activated and activated characters of the two processes. Contrarily to expectations, the present study, that reproduces the experimental reactivity, shows that dissociation is indeed non-activated in both surfaces.

Metal surfaces are effective chemical agents capable of adsorbing and/or dissociating molecules impinging from the gas phase, among other processes. Chemical reactivity on a surface depends on numerous factors, including temperature and pressure conditions. There is also an intrinsic feature of the metal surface that can play a dramatic role in its chemical activity, namely the crystal surface structure. An emblematic example of this is the dissociation of nitrogen molecules on tungsten surfaces. While dissociation is considerable for vanishingly small beam energy on the W(100) surface[1,2], it is roughly two orders of magnitude smaller at T=800K on the W(110) face[3,4] (see Figure 1).

It has been shown[5] that the high reactivity on the (100) surface is associated with the fact that the N_2/W(100) system is non activated, i.e., there exist paths leading to dissociation without any energy barrier. The efficiency of dissociation in this case is due to dynamic trapping: when approaching the surface, energy is transferred from perpendicular motion to other degrees of freedom so that the molecule cannot "climb" back the potential slope toward vacuum. On the (110) surface of W, however, the dissociation probability curve shows a S-like behavior. The probability is practically zero at low incidence energies and then increases with the incidence energy in two steps, first rather quickly and next smoothly until reaching a saturation value[3,6,7]. This behavior is usually associated with an activated system, i.e., no path leads to dissociation without overcoming a energy barrier. According to this picture, the unequal role of the (100) and (110) faces of W on the dissociation of low energy N_2 molecules would be a direct consequence of the activated and non-activated characters, respectively, of the two processes.

The difference in reactivity between the two faces arises from the long-distance surface-molecule interaction and not from the properties of a precursor well or those of the final atomic adsorption sites.

1 Donostia International Physics Center, San Sebastián, Spain **2** Centro de Física de Materiales-CSIC, UPV/EHU, San Sebastián, Spain **3** Universidad Nacional de Rosario, Rosario, Argentina

Published in **PRL**

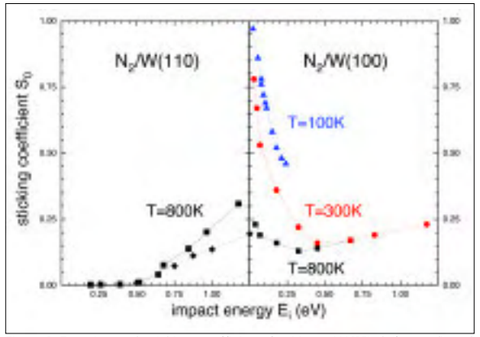

Figure 1: Experimental sticking coefficient for N_2 on W(110) (left panel) and W(100) (right panel) as a function of the molecular incidence energy. Data are extracted from References [1,2] for W(100) and from [3,4] for W(110).

Classical dynamics calculations performed on an *ab initio* six dimensional potential energy surface that describes the molecule surface interaction, have recently contravened this picture. Dissociation is non-activated on both surfaces. The striking difference in reactivity between the two faces is neither a consequence of the final state in the chemisorption process, a factor that is often stressed for these reactions. The big difference in the dissociation probability arises from the characteristics of the potential energy surface in the entrance channel, i.e., at large distances from the surface. The access to the precursor well, from which dissociation may eventually take place, is possible in the (110) surface for just a small number of trajectories while it is widely open in the (100) surface (see Figure 2). This strong influence of the long-distance interaction on surface reactivity introduces an unconventional and alternative view on the mechanisms driving gas/surface reaction dynamics in the thermal energy range, precisely the regime under which most technological applications are conducted.

[1] C.T. Rettner, E.K. Schweizer, H. Stein, and D.J. Auerbach, Phys. Rev. Lett. **61**, 986 (1988); C.T. Rettner, H. Stein, and E.K. Schweizer, J. Chem. Phys. **89**, 3337 (1988).
[2] M. Beutl, K.D. Rendulic, and G.R. Castro, Surf. Sci. **385**, 97 (1997).
[3] H.E. Pfnür, C.T. Rettner, J. Lee, R. J. Madix, and D. J. Auerbach, J. Chem. Phys. **85**, 7452 (1986).
[4] C.T. Rettner, E.K. Schweizer, and H. Stein, J. Chem. Phys. **93**, 1442 (1990).
[5] G. Volpilhac and A. Salin, Surf. Sci., **556**, 129 (2004).
[6] M. Alducin, R. Díez Muiño, H.F. Busnengo, and A. Salin, J. of Chem. Phys. **125**, 144705 (2006).
[7] M. Alducin, R. Díez Muiño, H.F. Busnengo, and A. Salin, Phys. Rev. Lett. **97**, 056102 (2006).

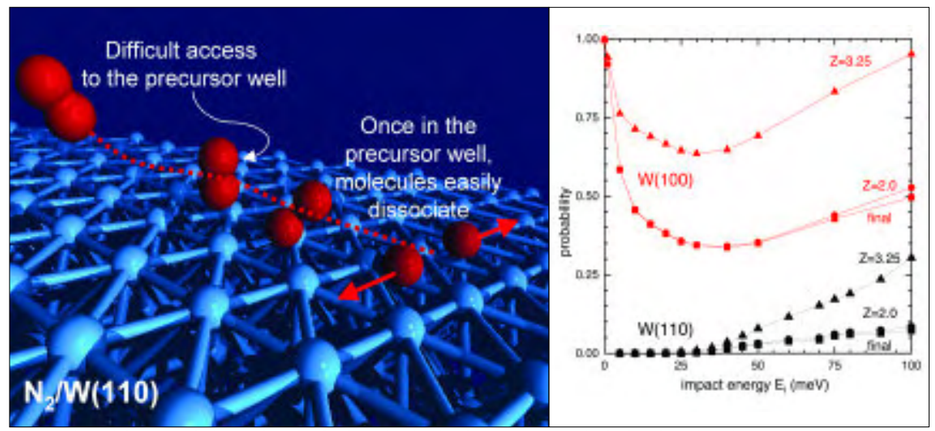

Figure 2: Classical dynamics calculations show that for thermal molecules, dissociation proceed in both surfaces through a precursor well in which molecules are temporally trapped. The low reactivity on the W(110) surface is simply a consequence of the small number of trajectories that can access the well. As a result, the dissociating probability is practically determined by the probability of the molecules to get closer than 3Å from the surface. This is shown in the right panel that compares the probabilities to reach Z=3.25 Å and Z=2.0 Å with the final sticking probability for both surfaces, W(100) and W(110).

Universal Features of Hydration Water Dynamics in Solutions of Polymers, Biopolymers and Glass-Forming Materials

S. Cerveny[1], A. Alegría[2], and J. Colmenero[1,2,3]

Water has physical and chemical properties essential for life since, besides stabilizing the biological structure; it enables bio-molecular motions and biological reactions. Therefore, it is of central importance to investigate the dynamics of water associated with biomolecules. Here, we report a set of 20 different water mixtures with very different hydrophilic substances. The temperature dependence of the water relaxation times exhibits a crossover from non-Arrhenius to Arrhenius behavior at the T_g-range of all the mixtures investigated so far. More interestingly, the temperature dependence of the relaxation times presents universal features both above and below the crossover temperature.

The behavior of water closely associated to—or restricted by—other molecules and systems is a subject of very active research. The main driving force for these studies is that water in cells and living organisms is always linked to proteins and other bio-molecules and hydration seems to play a decisive role controlling the structure, stability and function of these systems. Thereby understanding hydrated sys-tems in general and how the dynamics of water affects or control the properties of these systems are emerging questions of utmost importance.

In relatively rich water mixtures (typically between 20 and 50% wt. water content), by dielectric spectroscopy, water dynamics shows two relaxation processes in the low temperature range (130K–250K), provided water crystallization is avoided (see Figure 1 for fructose/water solutions). Process I was considered to be due to the cooperative rearrangement of the whole system whereas the faster process II has usually been associated to the reorientation of water molecules in the solution.

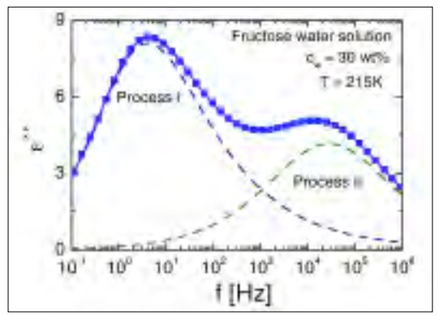

Figure 1: Loss component, ε´´, of the complex permittivity of fructose-water solution at 215K.

1 Centro de Física de Materiales-CSIC, UPV/EHU **2** Departamento de Física de Materiales, UPV/EHU, San Sebastián, Spain **3** Donostia International Physics Center, San Sebastián, Spain

Our recent work confirms that in all these solutions (see Figure 2), the temperature dependence of the relaxation times corresponding to Process II exhibit a crossover from a non-Arrhenius behavior towards and Arrhenius dependence in the temperature range where differential scanning calorimetry shows the global glass transition (T_g). This result can be interpreted in the following way. When the temperature is decreased towards T_g, the global dynamics becomes frozen but water molecules still have a significant mobility to be detected. Below T_g, water molecules are in some way trapped in a frozen matrix and thereby their motions have to be restricted. As a consequence, the temperature dependence of the relaxation times is Arrhenius like.

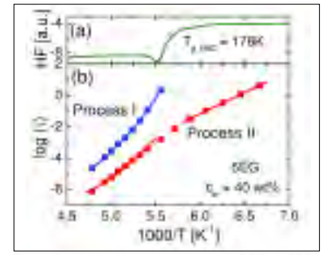

Figure 2: (a) Heat flow measured by DSC of 5EG-water solution during heating at a rate of 10K/min. (b) Temperature dependence of the relaxation times on 5EG-water solution.

Water dynamics presents universal features both above and below the glass transition temperature.

When we compared the Arrhenius temperature dependence of water dynamics in the glassy state for all systems here considered we found very similar activation energies. An almost constant value E_a = (0.54 ff10.04) eV can be deduced. This implies that a master curve for the temperature dependence of water dynamic below the crossover temperature could be obtained by properly shifting the relaxation times of all systems in the Y-axis. The master curve so obtained is shown in Figure 3 and summarizes the universal behavior of water dynamics in twenty systems of very different nature.

On the other hand, we can ask what the situation is concerning the temperature dependence of process II above the glass-transition of the system. In this range, the mixture is in a supercooled liquid like state and thereby the temperature dependence of the relaxation times is non-Arrhenius as it has already been mentioned. Astonishingly, the data in this range corresponding to all systems here considered can also be collapsed onto a new master curve. This is shown in Figure 4. This finding evidences that the universality of the temperature dependence of water dynamics in (relative rich) mixtures with hydrophilic substances holds both below and above the crossover range.

S. Cerveny, A. Alegría, J. Colmenero, Phys. Rev. Lett. (2006); Phys. Rev. E (2008).

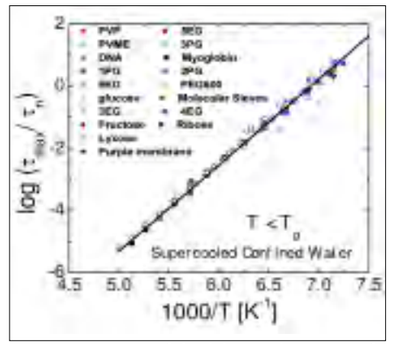

Figure 3: Master curve of the dielectric relaxation time for water dynamics in a wide variety of systems at temperature lower than T_g.

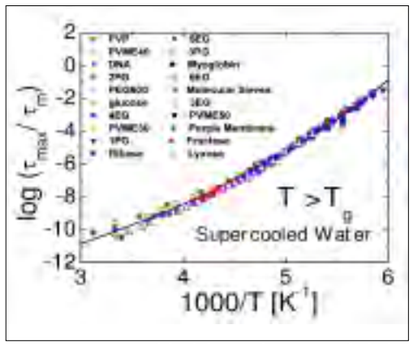

Figure 4: Master curve of the dielectric relaxation time for hydration water dynamic in a wide variety of systems at temperature higher than T_g.

Published in **Macromol**

Fluctuating Ripples on Nano-Sized Polymer Droplets

R. Lund[1], L. Willner[2], A. Alegría[3], D. Richter[2] and J. Colmenero[1,3]

Well-defined soft crystals can be formed by spontaneous self-assembly of block copolymers resulting in an array of spherical or cylindrical structures with sizes of the order of only some nano-meters. We demonstrate that using simple dynamical methods, very detailed structural information can be obtained, revealing that the properties of polymers confined in such droplets are strongly influenced by ripples on the interface—similar to fluctuating waves that can be observed on the surface of a quiescent sea or a lake.

Block Copolymers are made of two distinct polymer blocks covalently linked together. Once the blocks feel at least a slight mutual repulsion, such systems are able to self-assembly into well-defined soft structures—even crystals—where the entities making up the structures have a typical size in the nano-meter (nm) range. Interestingly, both the size and geometry of such systems can be conveniently tuned by changing the block composition, block length of the polymer and—to a certain degree—more straight forwardly by changing simple parameters such as temperature and pressure.

Because of these properties, block copolymers are very attractive systems for both fundamental studies and for practical applications, such as nanolithography, photonic crystals and other new tailor-made advanced materials. From a fundamental point of view, block copolymer self-assembly is interesting in itself and as templates for confined polymers, i.e. for understanding the effects of reducing the sample volume to the order of some nano-meters.

In this study we have performed a systematic selective investigation of the dynamics of poly(isoprene) (PI) in self-assembled asymmetric poly(isoprene)-poly(dimethylsiloxane) (PI-PDMS) block copolymer melts by employing Broadband Dielectric Spectroscopy (BDS) and Small Angle X-ray Scattering (SAXS). The structural investigations performed by SAXS, showed that the structures formed were either hexagonally ordered cylinders or close packed spheres (fcc/bcc). The size (radius) was in the range of 5 nm for the lowest molecular weight, 10 nm for the intermediate and 12.5 nm for the highest molecular weight.

The results from BDS of the three PI-PDMS block copolymers compared with the response of the corresponding PI homopolymers (having exactly the same molecular weight), are given in Figure 1. Two peaks are prominent; a low frequency response characterizing the relaxation of the end-to-end vector, i.e. the global relaxation; while a broader peak is visible at higher frequencies. This high frequency peak reflects the local segmental relaxation—also known as the α-relaxation responsible for the glass transition process.

Simple dynamical methods can yield highly detailed structural information of nano-segregated block copolymer melts.

1 Donostia International Physics Center, San Sebastián, Spain **2** Institute of Solid State Research, Forschungszentrum Jülich, Germany **3** Centro de Física de Materiales-CSIC, UPV/EHU, San Sebastián, Spain

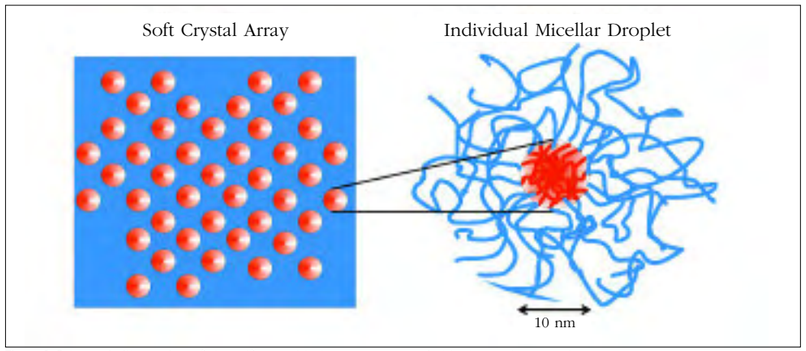

Figure 1: Schematic illustration of the self-assembled nano-structures in block copolymer melts.

The dynamics of block copolymers under soft confinement is strongly influenced by capillary wave fluctuations.

Interestingly, comparing the response from diblock copolymer with that of the homopolymer, we see that for all molecular weights, PI confined in the nanoscopic domains display a significant shift and broadening towards higher frequencies relative to the homopolymer state. This implies that the polymer dynamics speeds up and becomes more heterogeneous under such confinements.

An explanation of this behavior can be posed by considering fluctuations on the interface between PI and PDMS domains. Such a phenomenon is similar to the ripples observed on water surfaces and is a result of entropic forces and stochastic thermal fluctuations. This leads to an intermixing of the polymer segments and hence a heterogeneous local environment.

Taking these effects into account we can develop a model[1] where the gradient of local mobilities is given by a distribution of glass transition temperatures, T_g. This distribution of T_g can be calculated from the classical work of Helfand and Tegami (H-T)[2] for polymeric interfaces combined with the self-concentration concept originally introduced for miscible polymer melts by Lodge & McLeish[3]. Applying this model to the full BDS spectra, we obtain excellent fits as observed in Figure 2. From the fits we extract interfacial widths of 1.6-2.3 nm. These values nicely compare with values that can be estimated based on the H-T theory and classical capillary wave theory: 1.9-2.2 nm.

In summary, this study has demonstrated the importance of interfacial fluctuations on even local segmental polymer dynamics in nano-structured block copolymer melts. It also shows how simple dielectric spectroscopy experiments can provide very accurate structural information of interfaces—something that is difficult to achieve even with highly sensitive scattering techniques.

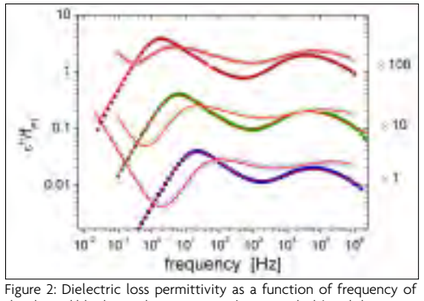

Figure 2: Dielectric loss permittivity as a function of frequency of the three diblock copolymer systems (open symbols) and the corresponding homopolymer references (filled symbols) at 243.15 K. The molecular weights of PI are 9000, 6000 and 4000 g/mole from top to bottom (shifted by the constant factor indicated).

[1] R. Lund, L.Willner, A. Alegría, J. Colmenero, and D. Richter, Macromolecules (Communication to the Editor) (2008), In Press.
[2] E. Helfand, Y. Tegami, J. Chem. Phys. **56**, 3592 (1972).
[3] T.P. Lodge and T.C.B. McLeish, Macromolecules **33**, 5278 (2000).

Polymer at the Glass Transition: Relaxation Needs Neighbors

D. Cangialosi[1], A. Alegría[1,2], and J. Colmenero[1,2,3]

The molecular motion in a polymer becomes increasingly sluggish when approaching the glass transition from above. To rationalise the motion of polymer segments in such a sluggish environment, the concept of cooperativity has been invoked. We provide a route to evaluate the length scale associated to such a cooperative region. To do so we combine the Adam-Gibbs theory of the glass transition with the self-concentration concept. The resulting length scale is between 1-3 nm depending on the glass-forming polymer.

The nature of the glass transition is one of the most important unsolved problems in condensed matter physics. Among the peculiar phenomena displayed by glass-forming liquids, the abrupt increase of the structural correlation time with decreasing temperature is one of the most intriguing. In this framework, more than 40 years ago Adam and Gibbs[1] theorized that such a pronounced temperature dependence is due to a cooperative process involving several basic structural units forming cooperatively rearranging regions (CRR), which size increases with decreasing temperature.

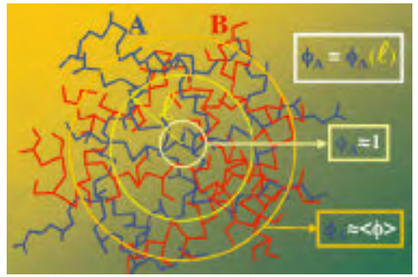

Figure 1: Schematic illustration of the self-concentration concept.

To determine the size of such CRR, we have incorporated the concept of self-concentration in the AG theory to polymer blends and polymer-mixture. The concept of self-concentration can be explained as follows (see Figure 1): when a volume is centred on the basic structural unit of the polymers of the mixture, the effective concentration ($\varnothing_{eff}$) will be larger than the macroscopic one ($\varnothing$). If the typical length scale associated to a relaxational process is such that $\varnothing_{eff}$ is larger than $\varnothing$, the dynamics will be intermediate between that of the pure polymer and the average dynamics of the mixture. This is the case for the length scale associated to the glass transition. Thus the self-concentration concept constitutes an extremely sensitive tool when exploring length scales of the order of those expected for CRR.

Starting from these premises we have developed a model combining the AG theory with the self-concentration concept[1]. The model relies on the fitting of just one parameter (α), namely the proportionality constant between the cooperative length scale and the configurational entropy. The latter is a central parameter in the AG theory as its decrease with decreasing temperature controls the increase

1 Centro de Física de Materiales-CSIC, UPV/EHU, San Sebastián, Spain **2** Departamento de Física de Materiales, Facultad de Química, Universidad del País Vasco (UPV/EHU), San Sebastián, Spain **3** Donostia International Physics Center, San Sebastián, Spain

Published in **PhysRevE**

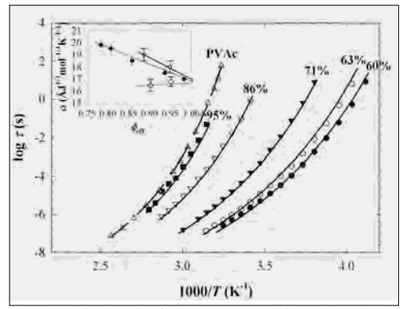

Figure 2: Arrhenius plot for PVAc segmental dynamics in PVAc/toluene systems and pure PVAc. The solid lines are the fits of the model. Inset: Variation of the α parameter with the average effective concentration of PVAc in various environments. The solid lines are linear fits to experimental data.

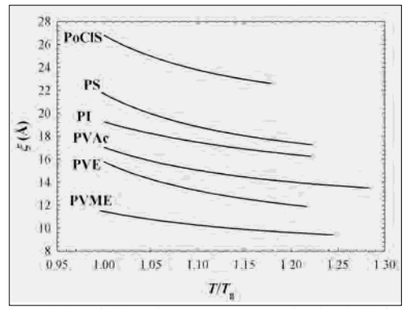

Figure 3: Size of CRR vs. the temperature normalized at the Tg for all investigated polymers.

of both the relaxation time, observed experimentally, and the cooperative length scale. The configurational entropy can be obtained from standard calorimetric measurements. As the only unknown parameter is polymer specific, its knowledge allows extracting the cooperative length scale of glass-forming polymers.

To measure the segmental dynamics we have employed broadband dielectric spectroscopy (BDS). Precise determination of the specific heat of the pure components of the blends has been performed by modulated differential scanning calorimetry (MDSC).

As an example, we show in Figure 2 the segmental dynamics of poly(vinyl acetate) (PVAc) in toluene. The two glass-formers display a rather large dynamic contrast being the glass transition temperature (T_g) of PVAc equal to 304K and that of toluene equal to 117K. Moreover, being all mixtures highly concentrated in PVAc, the dielectric response can be attributed to the segmental relaxation of PVAc in the mixture. From inspection of Figure 2, we clearly observe that the dynamics of PVAc is accelerated by the presence of the more mobile toluene. The acceleration is enhanced for blend with larger toluene content. These qualitative results are quantitatively captured by our model as indicated by the solid lines in Figure 2. The parameter α obtained from the fitting of the model is reported in the inset of Figure 2. Extrapolating to 100% PVAc allows obtaining the polymer specific α parameter.

Figure 3 displays the cooperative length scale, obtained from the knowledge of α, as a function of temperature for several polymers. This length is between 1 and 3 nm for all polymers under consideration and, notably, is correlated with the flexibility of the polymer being larger for the most rigid one. This result implies a possible connection between the cooperative length scale and the inter-chain distance, which might be universal in glass-forming polymers[2].

[1] D. Cangialosi, G.A. Schwartz, A. Alegría, J. Colmenero, J. Chem. Phys. **123**, 144908 (2005).
[2] D. Cangialosi, A. Alegría, J. Colmenero, Phys. Rev. E **76**, 011514 (2007).

The "self-concentration" concentration concept can be successfully exploited to determine the characteristic length scale associated to the glass transition.

Published in **PRL**

Infrared Imaging of Single Nanoparticles via Strong Field Enhancement in a Scanning Nanogap

A. Cvitkovic[1,2], N. Ocelic[1], J. Aizpurua[3], R. Guckenberger[2], and R. Hillenbrand[1]

We demonstrate nanoscale resolved infrared imaging of single nanoparticles employing near-field coupling in the nanoscopic gap between the metal tip of a scattering-type near-field optical microscope and the substrate supporting the particles. Experimental and theoretical evidence is provided that highly reflecting or polariton-resonant substrates strongly enhance the near-field optical particle contrast. Using Si substrates we succeeded in detecting Au particles as small as 8 nm (λ/1000) at midinfrared wavelengths of about ~10 μm. Our results open the door to infrared spectroscopy of individual nanoparticles, nanocrystals, or macromolecules.

Optical antennas such as plasmon resonant metal particles, engineered micro- and nanostructures or scanning probe tips allow for efficient conversion of propagating light into nanoscale-confined (and strongly enhanced) optical fields. They are therefore the key elements in the development of highly sensitive optical (bio)sensors, nanoscale resolution near-field optical microscopy[1] and infrared nanospectroscopy. The local field-enhancement can be significantly increased by optical near-field coupling of such (nano)structures separated by a nanoscopic gap. To cite some examples, extraordinary high optical field enhancements inside nanogaps allow for single molecule Raman spectroscopy, two-photon excited photoluminescence or white-light super-continuum generation[2]. Moreover, the interest to operate at infrared frequencies is motivated by the fascinating prospects of performing direct vibrational spectroscopy for chemical identification of individual nanoscale objects.

Here we demonstrate a simple but efficient optical microscopy concept that exploits the strong field enhancement in a scanning nano-gap for highly sensitive and nanoscale resolved optical imaging. It is realized by a scattering-type near-field microscope (s-SNOM) where imaging is performed by recording light scattering from optical probes like metal nanoparticles or metal tips (Figure 1(a)). Usually, the objects to be imaged are adsorbed on a low-dielectric substrate (e.g. glass) and the near-field coupling between tip and substrate is weak. By employing highly reflecting substrates, the near-field optical contrast of nanoscale objects can be strongly enhanced. The application of this improved near-field optical tip-substrate coupling to generate both strongly enhanced and confined optical fields, enables for the first time infrared microscopy of single gold nanoparticles with diameters d_{Au} as small as 8 nm (λ/1000) at wavelengths of about ~10 μm. The extremely weak scattering cross section C_{sca} of the particles at this wavelength (C_{sca}<10^{-20} cm^2) due to the scaling $C_{sca} \propto d^6/\lambda^4$ prevented infrared analysis of single nanoparticles up to date, as the signals vanished far below the background level. With use of the scanning-nanogap configuration presented here, we overcome this limitation. A series of experiments with Au nanoparticles show that the use of a substrate with a "tuned" optical response provides significant improvement both in absolute signal and contrast of the nanoparticles. Three different types of substrates are used: (i) a weak dielectric such as SiC at 1080 cm-1 (ε≈3), (ii) a nearly perfectly conducting mirror (ε≈-5000+1000i) and (iii) a phonon-polariton resonant substrate, such as SiC at 927cm-1 (ε≈-2). The improvement in signal and contrast for the latter can be observed in Figure 1(b) and (c). This effect is explained by the strong near-field coupling between tip apex and substrate yielding highly concentrated optical fields in the gap for probing the objects.

1 Nano-Photonics Group, Max-Planck-Institut für Biochemie, Martinsried, Germany **2** Abteilung Molekulare Strukturbiologie, Max-Planck-Institut für Biochemie, Martinsried, Germany **3** Donostia International Physics Center, San Sebastián, Spain

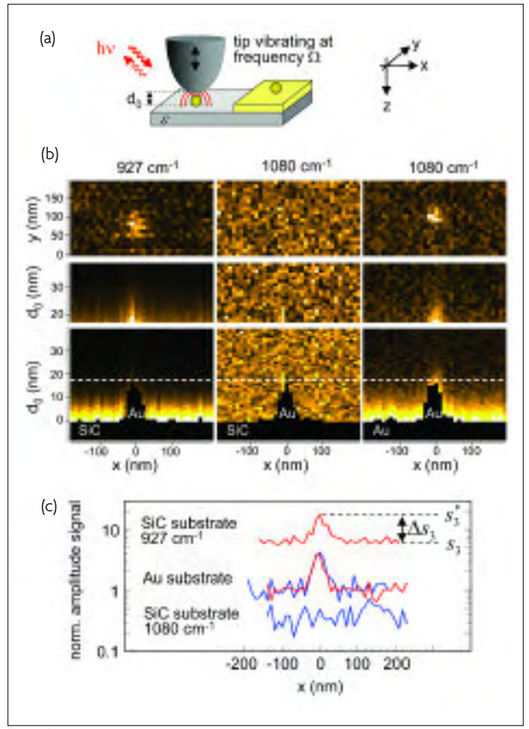

Figure 1

To support the experimental findings, we perform full electrodynamic calculations of the electromagnetic field enhancement at the scanning nanocavity with and without the presence of the particle for a perfectly conductive substrate and for a resonant substrate. We first calculate the near-field distribution for a Pt-tip above a Au surface showing field concentration at the tip apex (Figure 2(a)). Due to the near-field coupling with the Au mirror the fields are enhanced by a factor of 4 compared to an isolated tip. In case a Au particle is placed inside the gap the fields increase by another factor of 5 (Figure 2(b)). The main spots of enhancement are thereby located at the particle-substrate and particle-tip junctions. Replacing the Au mirror by a SiC substrate the excitation of phonon-polaritons in the SiC further increases the near-field coupling which additionally enhances the fields by a factor of about 10 (Figure 2(c)). This enhancing effect is totally consistent with the experimental findings.

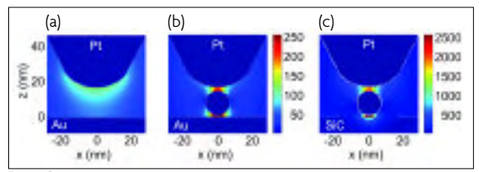

Figure 2

The tip-substrate coupling in scattering-type near-field optical microscopy presented here enables for the first time nanoscale resolved infrared imaging of nanoparticles even below 10 nm in diameter. The near-field optical particle contrast can be strongly enhanced by highly reflecting substrates such as Au and Si. Particularly strong particle contrasts are achieved by resonant near-field coupling provided, for example, by phonon-polariton excitation in a SiC substrate. These results open the door to a variety of applications in high-resolution imaging of nanoscale objects (e.g. gold biolabels) and in infrared near-field spectroscopy of thin films and organic as well as biological nanoparticles[3].

[1] R. Hillenbrand and F. Keilmann, Physical Review Letters **85**, 3029 (2000).
[2] P. Mühlschlegel, H.-J. Eisler, O. J. F. Martin, et al., Science **308**, 1607 (2005).
[3] M. Brehm et al, Nano Letters **6**, 1307 (2006).

10 nm gold nanoparticles resolved with infrared light.

Do Real Polymers Fit in the Mode Coupling Theory?

J. Colmenero[1,2,3], A. Narros[3], F. Álvarez[2,3], A. Arbe[2], and A.J. Moreno[1]

Fully atomistic simulations reveal localized motions (Johari-Goldstein processes), in addition to the diffusive structural α-relaxation, in a common polymer, 1,4-polybutadiene. The former local processes occur in the time window where the *β*-process of the Mode Coupling Theory (MCT) is expected. We show that the application of MCT is still possible, yielding unusual values for the associated dynamic exponents. This result might originate from the coexistence of two mechanisms for dynamic arrest in polymers: intermolecular packing and intramolecular barriers for local conformational changes.

The Mode Coupling Theory (MCT) is probably the most ambitious approach to the glass transition problem. A mean-field factorization for density fluctuations entering the memory kernel in a Mori-Zwanzig equation provides a closed set of coupled non-linear equations for density correlators. The only external input is the static structure factors, which can be obtained from simulations or experiments. In the case of simple glass-formers (the archetype being the hard sphere fluid) the latter can be directly derived from the interaction potential through liquid state theories. Hence, MCT constitutes a first-principle theory of the dynamic arrest associated to the glass transition. MCT predicts a kinetic transition to a non-ergodic ('glassy') state at a critical temperature T_c. This transition is manifested in density correlators by a jump of their long-time limit from zero to a finite value. Due to the mean-field character of the MCT factorization, T_c overestimates kinetic arrest and the real glass transition actually occurs at lower temperature. MCT predictions for the α-structural relaxation break down very close to T_c and below. Still, the shape of glass transition lines in the space of control parameters are often qualitatively reproduced by the T_c-lines. The actual success of MCT lies in the derivation, from first-principles, of highly non-trivial features as re-entrant glass transitions, roto-translational decoupling, sublinear diffusion, logarithmic relaxation, dynamic demixing, or decoupling between self- and collective motions. It also establishes a set of scaling asymptotic laws for density correlators and relaxation times at temperatures above T_c. The associated dynamic exponents are univocally related to a single one ($\lambda \leq 1$). The latter parameter is also univocally determined by static correlations at T_c.

MCT constitutes a first-principle theory of the glass transition.

1 Donostia International Physics Center, San Sebastián, Spain **2** Centro de Física de Materiales-CSIC, UPV/EHU, San Sebastián, Spain **3** Departamento de Física de Materiales, UPV/EHU, San Sebastián, Spain

Published in **JPhys**

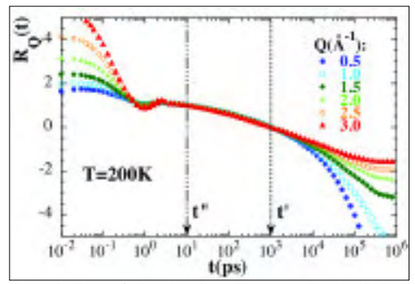

Figure 1: Test of the *β*-scaling. The ratio $R_Q(t)= [F_S(Q,t)-F_S(Q,t')]/[F_S(Q,t)-F_S(Q,t^*)]$, where $F_S(Q,t)$ is the density self-correlator of hydrogens, is independent on the wave vector Q.

MCT predictions are not altered by the presence of Johari-Goldstein processes.

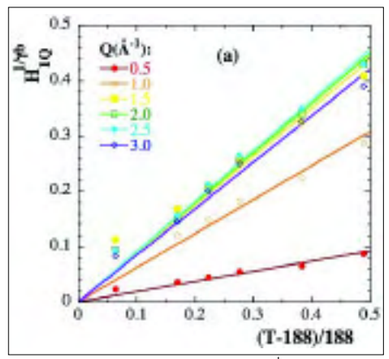

Figure 2: Test of the power law $H_{IQ} \propto (T-T_c)^{1/b}$, for the prefactor of the von Schweidler regime of the *β*-process: $F_S(Q,t) = f_Q - H_{IQ} t^b + O(t^{2b})$. The dynamic exponents γ and b yield univocally $\lambda = 0.93$.

Derivation of dynamic exponents by solution of MCT equations is in practice only possible for rather simplified models of glass-formers (spheres, ellipsoids, rigid water, bead-spring chains...). The complexity of MCT equations grows up exponentially when trying to incorporate the detailed molecular structure. However, the mentioned scaling predictions are not altered if the structure of the equations still belongs to the same class. For complex systems, the corresponding MCT dynamic exponents are derived as fit parameters. Consistency requires the so-obtained exponents to be univocally related to a unique value of λ.

In this work we have performed an exhaustive test of MCT scaling predictions on simulation results of a fully atomistic model for a common polymer, 1,4-polybutadiene. The force field includes a detailed description of characteristic intrachain motions (bond stretching, angle bending, dihedral angle torsion...). Simulations reveal *localized* motions (Johari-Goldstein processes), in addition to the *diffusive* structural α-relaxation. The former local processes correspond to conformational transitions driven by intramolecular barriers, and occur in the same time window for which MCT predicts the *β*-process. The latter is *a priori* not related to the Johari-Goldstein process: it corresponds to the temporary trapping of each particle by its neighbors prior to the α-process, which leads to the final structural relaxation.

The presence of Johari-Goldstein processes might question the applicability of MCT in real polymers. However, a full and consistent description of scaling behavior with a single λ-parameter is achieved. Figures 1 and 2 show some illustrative tests of scaling predictions. Hence we conclude that MCT predictions are not altered by the presence of Johari-Goldstein processes. An unusually large value $\lambda = 0.93$ is obtained, close to the upper limit $\lambda = 1$. In the framework of MCT large λ-values arise in systems with coexisting mechanisms for dynamic arrest. In real polymers such mechanisms would be intermolecular packing, and intramolecular barriers for local conformational changes. The latter are not present in simplified bead-spring models for polymers, for which solution of MCT equations provides a standard value $\lambda = 0.72$. Results presented here open new perspectives for the application of MCT in complex materials.

J. Colmenero, A. Narros, F. Alvarez, A. Arbe, and A.J. Moreno, J. Phys.: Condens. Matter **19**, 205127 (2007)

Miscible Polymer Blends with Large Dynamical Asymmetry: A New Class of Solid State Electrolytes?

D. Cangialosi[1], A. Alegría[1,2], and J. Colmenero[1,2,3]

PVME/PS/$LiClO_4$ systems were investigated with the aim of obtaining mechanically solid materials with high conductivity. It was found that the crossover from super-Arrhenius to Arrhenius temperature dependence, found for the PVME relaxation time in PS and attributed to confinement, also manifests for the ionic conductivity. This implies that for some structurally solid blends the ionic conductivity is of the same order of those of liquid PVME. This means that miscible polymer blends represent appealing candidates as solid state electrolytes.

Investigation in the field of solid state ionics has been recently the subject of intense research. Strong interest in this field has been driven by the appealing idea of obtaining materials with the mechanical properties of a solid and the ionic conductivity of a liquid. In this respect polymer nanocomposites, have been widely studied in recent years. This is due to the double nature of these materials: liquid for what concerns the ionic conductivity and solid from a structural point of view.

In an attempt to introduce a new class of solid state electrolytes, we have investigated the ionic conductivity of a miscible polymer blend; i.e., poly(vinyl methyl ether)/polystyrene blend (PVME/PS). It presents a very large dynamical asymmetry; i.e. a large difference of glass transition temperature (T_g) between the two polymers: 249K for PVME and 373K for PS. Recent dielectric spectroscopy results on the dynamics of dilute PVME in PS highlight the presence of a low activation energy motion with Arrhenius-like behavior[1]. This relaxation, in analogy with polymer/nanocomposites systems, has been attributed to the restricted motion of PVME chains due to the presence of frozen PS as a consequence of the selective freezing-in occurring in miscible polymer blends. In particular, a crossover from a super-Arrhenius behavior; i.e. an increase of the apparent activation energy with decreasing temperature, at high temperature, normally observed in fragile glass-forming systems, to a milder Arrhenius temperature dependence is observed for PVME dynamics in PS.

Miscible polymer blends represent appealing candidates as solid state electrolytes.

1 Centro de Física de Materiales-CSIC, UPV/EHU, San Sebastián, Spain **2** Departamento de Física de Materiales, Facultad de Química, Universidad del País Vasco (UPV/EHU), San Sebastián, Spain **3** Donostia International Physics Center, San Sebastián, Spain

Published in **Macromol**

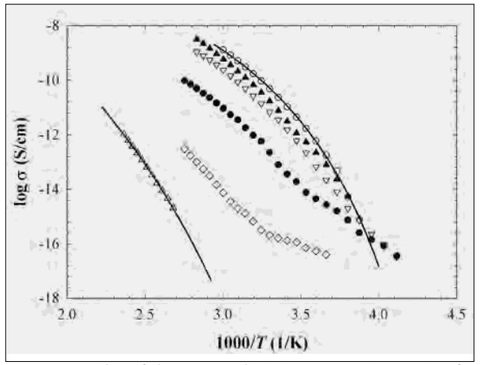

Figure 1: Logarithm of the ionic conductivity vs. inverse temperature for PVME/PS/LiClO4 systems with the following PVME weight percentages: 10% (empty diamonds); 20% (filled circles); 30% (empty down triangles); 50% (filled up triangles); for PS (empty up triangles) and PVME (empty circles). The solid lines are the fits through the VFT equation to PS and PVME experimental data.

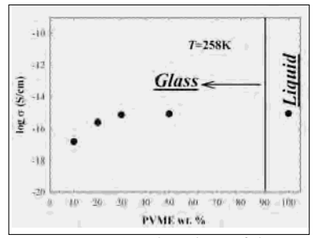

Figure 2: Composition dependence of the ionic conductivity at 258K.

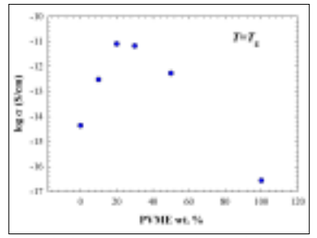

Figure 3: Composition dependence of the ionic conductivity at the T_g of each PVME/PS/$LiClO_4$ systems.

Miscible PVME/PS blends display ionic conductivities orders of magnitude larger than those of the pure polymers.

Starting from these premises, we have used broadband dielectric spectroscopy to study the ionic conductivities properties of PVME/PS blends as well as those of the pure polymers[2]. We have mostly focused on blends highly concentrated in PS; namely, those blends for which the effect of confinement on PVME is most prominent. Blends with 10, 20, 30 and 50% wt. PVME have been investigated. In addition, 1% wt. lithium perchlorate (LiClO4) has been added to all blends to improve the ionic conductivity and perform a straightforward comparison among their conductivities. Our results, shown in Figure 1, suggest that for blends with less than 30% wt. PVME a clear crossover from super-Arrhenius to Arrhenius temperature dependence of the ionic conductivity occurs, mimicking the behavior of PVME dynamics in PS[1]. This finding strongly supports the idea that charge transport essentially takes place along mobile paths within confined PVME chains. The main striking consequence of the crossover to a low temperature Arrhenius behavior implies that the ionic conductivity of some structurally glassy PVME/PS blends is comparable to that of pure liquid PVME, as shown in Figure 2 where the isothermal ionic conductivity is displayed as a function of PVME wt. %. In addition, comparing structurally analogous systems, we demonstrate that miscible PVME/PS blends display ionic conductivities orders of magnitude larger than those of the pure polymers. This is shown in Figure 3 where the ionic conductivity is presented as a function of PVME wt. % at the T_g.

All these results indicate that miscible polymer blends with large dynamical asymmetry may represent appealing candidates as solid state electrolytes in analogy with polymer nanocomposites. However, we emphasize here that, whereas polymer nanocomposites present serious technological drawbacks due to the necessity of obtaining intercalated nanocomposites rather than exfoliated or immiscible, in the case of polymer blends thermodynamic miscibility is the only requirement, apart from the large dynamical asymmetry.

[1] C. Lorthioir, A. Alegría, J. Colmenero, Phys. Rev. E **68**, 031805 (2003).
[2] D. Cangialosi, A. Alegría, J. Colmenero, Macromolecules (2008). In press.

Optical Cooling of Er-doped Solids

J. Fernández[1,2], A.J. García-Adeva[1], and R. Balda[1,2]

Lasers are commonly known as sources of heat—used to burn or cut through tissue and other materials, but when shined on certain solids doped with rare-earth ions, a laser can cool down the material. We have recently achieved this effect in certain solids doped with Er^{3+} ions at powers and wavelengths of the incident laser light reachable by conventional laser diodes, which opens a pathway toward developing small solid-state-refrigerators for dissipating heat in optical telecommunication optoelectronic devices.

The basic principle that anti-Stokes fluorescence might be used to cool a material was first postulated by P. Pringsheim in 1929. Twenty years later A. Kastler suggested that rare-earth-doped crystals might provide a way to obtain solid-state cooling by anti-Stokes emission (CASE). An anti-Stokes emission occurs when a material emits more energy than it absorbs. The key is to shine photons onto the material that fall short of the energy needed to excite the rare earth ions to a higher energy level. The material uses the energy from thermal vibrations to make up the difference. Whenever a quantum of these thermal vibrations is absorbed, an ion is excited to a higher energy state and then fluoresces, carrying energy out of the system and cooling the material. It was not until 1995 that the first solid-state CASE was convincingly proven by Epstein and coworkers in an ytterbium-doped heavy-metal fluoride glass. Since then on, just a few other systems, using the ions ytterbium and thulium, have been shown to cool via anti-Stokes emission. In most of the materials studied, the presence of nonradiative processes hindered the CASE performance. As a rule of thumb a negligible impurity parasitic absorption and near-unity quantum efficiency of the anti-Stokes emission from the rare-earth levels involved in the cooling process are required, so that nonradiative transition probabilities by multiphonon emission or whatever other heat generating process remain as low as possible.

Laser cooling of rare-earth-doped materials could have many applications. The simplest and probably most profitable one is for developing cryocoolers for the microprocessors of personal computers. Other important applications of this type of laser cooling are, for example, the development of radiation-balanced laser that use dual wavelength pumping to offset the heat generated by the pump laser. Also, this could have many applications in bioimaging and phototherapy, where this dual wavelength pumping could also partially offset the heat that could otherwise damage the living specimen under study.

Laser-cooled materials could be
a path to low temperature,
high efficiency, noiseless, vibration-less,
and inexpensive, optical refrigerators.

1 ETS Ingeniería de Bilbao-UPV/EHU, Bilbao, Spain **2** Centro de Física de Materiales-CSIC, UPV/EHU and Donostia International Physics Center, San Sebastián, Spain

Published in **PRL**

Unfortunately, these applications are still way ahead down the road so, in the meantime, a number of research groups are trying to investigate novel materials doped with different rare-earth ions amenable of efficient laser cooling. Erbium, in particular, has always been an attractive ion to researchers. Its excited energy state requires light 1.5 microns in wavelength, which is used in optical communications. But erbium has a more complicated electronic energy scheme than the other two ions, which made some researchers skeptical that anti-Stokes cooling could be achieved in erbium-doped materials.

In spite of these difficulties, our group recently demonstrated anti-Stokes laser cooling on two new low phonon materials doped with erbium which were synthesized in our laboratory: a potassium lead pentachloride and a heavy-metal fluorochloride glass. We focused a titanium-sapphire laser onto the samples and mapped the temperature with an infrared camera. The typical pictures taken by this device look like the ones shown in the insets of Figure 1 for the Er-doped crystal sample for two different times after irradiation started. The sample color changes between these two instants of time and that indicates a slight decrease of its temperature. The main part of this figure depicts the average temperature of the sample as a function of time. It is easy to see that this average temperature dropped by around 0.7º C after 25 minutes of laser irradiation. Interestingly, after those 25 minutes we shut off the laser and this shows up in this as an upturn in the temperature of the sample. Similar results are obtained for the glass sample, as shown in Figure 2. The drops in the average temperature were small: 0.7º C for the crystal and 0.5º C for the glass, but they have to be put into context: this was more like a proof of concept that these materials could be cooled. The Er concentrations were minute and no attempt was made to optimize the geometry of the experiment to maximize the cooling efficiency. The ultimate reason why this effect was achieved is that both the crystal and glass samples were extremely pure, which minimized the effect of background absorption processes that contribute to heating.

J. Fernández, A.J. García-Adeva, R. Balda, Physical Review Letters **97**, 033001 (2006).

Some lasers can burn through solids, but others,
shined on the right materials, have a cooling effect.

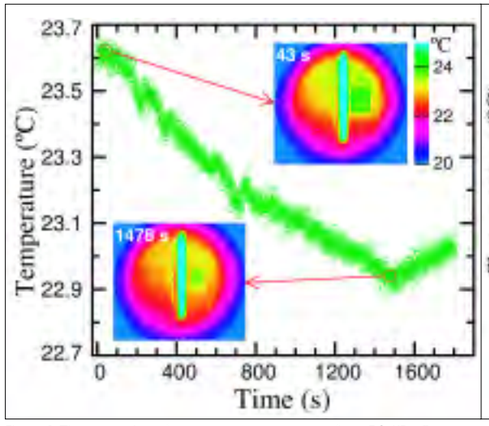

Figure. 1: Time evolution of the average temperature of the Er^{3+}:KPb_2Cl_5 sample at 870 nm. The insets show colormaps of the temperature field of the whole system (sample plus cryostat) at two different times as measured with the thermal camera. The rectangle in the upper inset delimits the area used for calculating the average temperature of the sample.

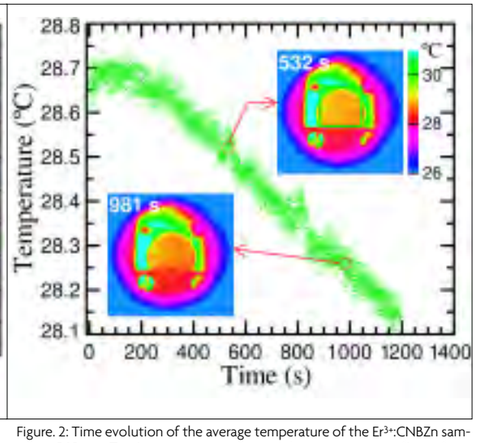

Figure. 2: Time evolution of the average temperature of the Er^{3+}:CNBZn sample at 860 nm. The insets show colormaps of the temperature field of the whole system (sample plus cryostat) at two different times as measured with the thermal camera. The rectangle in the upper inset delimits the area used for calculating the average temperature of the sample.

Predicting the Miscible Polymer Blends Dynamics Under Processing Conditions

G.A. Schwartz[1], A. Alegría[1,2] and J. Colmenero[1,2,3]

The increasing industrial use of polymer blends as well as their unique dynamical properties require knowing how the segmental dynamics of each polymer is affected by the other component. We have developed a model to describe the component segmental dynamics in miscible polymer blends as a function of pressure, temperature and composition. This allows predicting the component dynamical properties in the blends from the properties of the pure components in typical processing conditions. Furthermore, new insights on some fundamental aspects of polymer dynamics can be obtained from the model.

Polymer materials are suitable for a huge number of applications and are therefore found everywhere. A route commonly used to obtain new polymer materials is by mixing already existing polymers, which allows tuning the desired properties of the resulting material. Among the broad range of multicomponent polymer materials, a family of both, fundamental and technological interest is that of the binary miscible polymer blends. These systems are homogeneous mixtures of two different polymers; however, they present what is referred to as dynamical heterogeneity, i.e., two different dynamics are observed. This is due to the fact that in miscible polymer blends the local effective concentration of one component will, on average, be richer in that component compared to the bulk composition. This is a direct consequence of the chain connectivity and is one of the most important characteristics of the polymer blends dynamics.

On the other hand, it is important to note that the understanding of the molecular dynamics of polymers and polymer blends is hardly possible using temperature as the single thermodynamic variable. By varying temperature both thermal energy and density change and therefore their specific contribution becomes indistinguishable. By using pressure as an additional experimental variable, thermal and density contributions to the polymer dynamics can be decoupled. Thus, using temperature *and* pressure as experimental variables is of fundamental relevance for scientific as well as technological purposes.

Polymer blending is a convenient way to obtain new materials with tailor made properties.

1 Centro de Física de Materiales-CSIC, UPV/EHU, San Sebastián, Spain **2** Departamento de Física de Materiales, UPV/EHU, San Sebastián, Spain **3** Donostia International Physics Center, San Sebastián, Spain

Published in **JChemPhys**

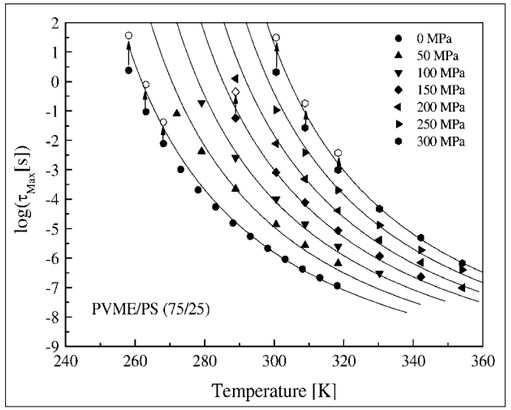

Relaxation time of PVME vs temperature at different pressures for PVME/PS (75/25). Filled symbols represent the experimental maximum relaxation times whereas open ones represent the estimated relaxation time of the average concentration. Solid lines represent the fit of the experimental data with the here proposed model.

If the only fitting parameter of our model can be determined by means of an independent experiment, the model would become completely predictive.

We have combined the concept of the chain connectivity with the Adam-Gibbs (AG) theory to develop a new model to describe the component segmental dynamics in miscible polymer blends as a function of pressure, temperature and composition[1]. The AG theory links the dynamics and thermodynamics behavior of polymers (and glass formers in general) by means of the configurational entropy (S_c) and has shown to be a very good approach to describe the molecular dynamics close (and above) the glass transition temperature (T_g). Conceptually, we propose for the dynamics of each polymer in athermal miscible blends to write the configurational entropy of each component as a linear combination of those of the pure polymers weighted by the effective concentration. This approach has shown to give an excellent description of the experimental data at atmospheric pressure[2].

In order to apply our model to a given polymer blend, it is first necessary to perform a full characterization of the pressure-temperature dynamics of both components of the blend. According to previous works[3] we have to perform DSC and PVT measurements on each of the neat components as well as to measure the relaxation times at atmospheric and higher pressures to calculate the corresponding parameters. This procedure gives the full temperature-pressure dependence of the segmental relaxation time for each component of the blend. Once the dynamics of the pure polymer is known we can use our model to describe the component segmental dynamics in the blend with only one fitting parameter.

In order to test our model we have measured the dielectric response of poly(vinyl methyl ether) (PVME) in a blend with poly(styrene) (PS). As an example, we show in the Figure the segmental relaxation time of PVME in PS at a concentration of 75% of PVME. The only fitting parameter of our model linearly decreases with increasing pressure for all PVME concentrations. As shown in the Figure the model gives an excellent description of the experimental data.

In contrast to previous models which need information about the blends, our model is able to describe the segmental dynamics of each component in the blend only from the knowledge of the dynamics of the pure polymers. Based on previous results[4] we expect that the only fitting parameter of our model can be determined by means of an independent experiment. If this is possible, our model will become completely predictive.

[1] G.A. Schwartz, A. Alegría and J. Colmenero, J. Chem. Phys. **127**, 154907 (2007).
[2] D. Cangialosi, G.A. Schwartz, A. Alegría and J. Colmenero, J. Chem. Phys. **123**, 144908 (2005).
[3] G.A. Schwartz, J. Colmenero and A. Alegría, Macromolecules **39**, 3931 (2006).
[4] G.A. Schwartz, D. Cangialosi, A. Alegría and J. Colmenero, J. Chem. Phys. **124**, 154904 (2006).

Hellman-Feynman Operator Sampling in Diffusion Monte Carlo Calculations

R. Gaudoin[1] and J.M. Pitarke[2,3]

Diffusion Monte Carlo calculations typically yield highly accurate results for the total energy in solid-state and quantum-chemical calculations. However, operators that do not commute with the Hamiltonian, such as the potential energy, are only sampled correctly up to second order in the error of the underlying trial wavefunction. Our method, based on the Hellman-Feynman theorem, is easy to implement and enables the correct sampling of a wide class of operators.

Diffusion Monte Carlo (DMC) is widely used for the computation of properties of solids and molecules[1]. Frequently, it is used as a check on other methods[2] or even as an input[3]. It is therefore very important that DMC be as accurate as possible. However, other than for the total energy, standard DMC calculations are not as definitive as one would hope, since operators that do not commute with the Hamiltonian cannot be sampled exactly within standard DMC. Hellman-Feynman sampling (HFS) is a simple yet effective addition to standard DMC that plugs that gap and is easy to implement.

From a mathematical point of view DMC samples operator expectation values with respect to the product of a given trial wavefunction and the ground-state within the nodes of that trail wavefunction, i.e. the fixed-node ground-state wavefunction. It turns out that for operators that commute with the Hamiltonian this is equivalent to sampling with respect to the square of the fixed-node ground-state wavefunction. This includes of course the Hamiltonian itself so the the DMC total energy is correct with respect to a given fixed nodal structure. The residual nodal error is small, hence the success of DMC for total-energy calculations.

However, there is a large class of important operators that do not commute with the Hamiltonian. This includes the density or the potential energy. In such cases, the DMC error is proportional to the error in the trial wavefunction. Employing a few tricks one can improve on this slightly. Nevertheless, due to the true many-body wavefunction being not only unknown but also difficult to approximate the residual error can remain disconcertingly large.

Keeping in mind that ultimately the DMC algorithm is nothing but a large sum that yields the total energy, we see the HF derivative can be applied ithout problem to the algorithm itself.

1 Donostia International Physics Center, San Sebastián, Spain 2 CIC nanoGUNE Consolider, San Sebastián, Spain 3 Materia Kondentsatuaren Fisika Saila, UPV/EHU, and Centro de Física Materiales-CSIC, UPV/EHU, Bilbao, Spain

Published in **PRL**

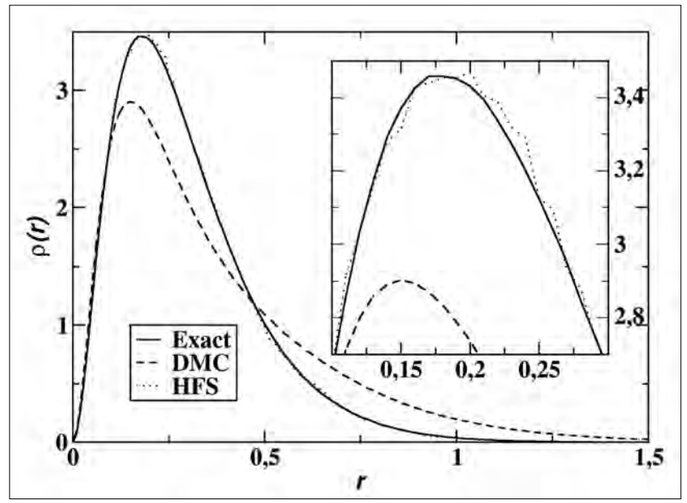

Writing down the DMC algorithm as a mathematical formula and applying the HF derivative to it yields an object that when sampled using standard DMC produces the exact operator expectation value. It has to by construction.

A widely used theorem in physics, the Hellman-Feynman theorem, is frequently used to express expectation values as derivatives of total energies. Our paper consists of a novel Quantum Monte Carlo application of this theorem. We know the DMC algorithm gets the total energy essentially right — we shall ignore the small residual fixed-node error. Furthermore, at the end of the day the DMC algorithm is just an equation, the total energy on one side, a large sum on the other. We apply the Hellmann-Feynmann derivative to that sum, i.e. the DMC algorithm. Interestingly, the result can be cast as the DMC sampling of a mathematical object, that, while derived from an observable, in itself is no such thing. That though does not matter as it only turns into an easily coded auxiliary variable and the rest of the DMC machinery can still be used as-is.

Our numerical tests show that this new method works well and also seems applicable to relatively large systems. E.g. in the figure we compare results for the Helium density ρ(r) using a skewed trial wavefunction. The standard DMC result clearly is wrong. In contrast, using the same bad input wavefunction, HFS, while somewhat noisy, reproduces the exact Helium density. The downside of HFS is the magnitude of the statistical noise which is larger than for standard sampling. Current research is underway to limit this and furthermore an extension of our analysis might yield a method for the DMC evaluation of response functions which currently is numerically not feasible.

[1] W.M.C. Foulkes, L. Mitas, R.J. Needs, and G. Rajagopal, Rev. Mod. Phys. **73**, 33 (2001).
[2] M. Nekovee and J.M. Pitarke, Comput. Physics Commun. **137**, 123 (2001).
[3] D.M. Ceperley and B.J. Alder, Phys. Rev. Lett. **45**, 566 (1980); See also R.M. Dreizler and E.K.U. Gross, *Density-Functional Theory. An Approach to the Quantum Many-Body Problem*, Springer, 1990.

Electronic Stopping Power in LiF From First Principles

J.M. Pruneda[1,2], D. Sanchez-Portal[3,4], A. Arnau[3,4,5], J.I. Juaristi[3,4,5], and E. Artacho[3,6]

Using first-principles simulations of the electronic structure, based on the time-dependent density-functional theory, we have calculated the rate of energy transfer from a moving proton and antiproton to the electrons of an insulating material, LiF. The electronic stopping power, i.e., the energy transferred to the electrons per unit path length, presents a threshold velocity of ~0.2a.u.. Consistent with recent experimental observations, the energy loss by protons becomes negligible below this value for LiF. We find that the projectile energy loss mechanism is observed to be extremely local and that results similar to those of the solid can be obtained using a minimal Li_6F^{5+} cluster.

The dramatic and slow death of Alexander Litvinenko, the ex soviet agent, after poisoning with tiny amounts of polonium, represents an example of the substantial damage produced in matter by ions shooting through it. In addition to its effect on living matter, this kind of damage is source of concern regarding the durability of materials designed for plasma containment in nuclear fusion, or of the ones used safely to host nuclear waste, hopefully for millions of years. Materials swell and crack when subjected to such ordeals, but they do it differently depending on their chemical nature. Theoretical simulations complementing indirect experiments are extremely important to understand and successfully predict these behaviors, given the fact that direct experimentation over millions of years exceeds the duration of a PhD project in most universities. A key for these simulations is the knowledge of the way hot electrons get in matter while a projectile traverses it, since that crucially determines how atoms interact with each other, and thus the response of matter. The rate of this energy uptake by electrons depends on the speed of the projectile. It happens to be very poorly characterised for insulating matter at relatively low velocities due to experimental difficulties. So much so, that even the fact on whether there is a velocity threshold is unclear, meaning whether the energy transfer is quite suppressed below a given velocity. This is critical for the ceramic materials proposed for nuclear waste containment: the velocity of typical decaying nuclei happens to be very much around the hypothetical thresholds for these materials.

How “hot” electrons get in a crystal when a projectile traverses it is crucial to determine the response of matter to radiation.

1 Instituto de Ciencia de Materiales de Barcelona-CSIC, Bellaterra, Spain **2** Department of Physics, University of California, Berkeley, California, USA **3** Donostia International Physics Center, San Sebastián, Spain **4** Centro de Física de Materiales-CSIC, UPV/EHU, San Sebastián, Spain **5** Departamento de Física de Materiales, Facultad de Química, San Sebastián, Spain **6** Department of Earth Sciences, University of Cambridge, UK

Published in **PRL**

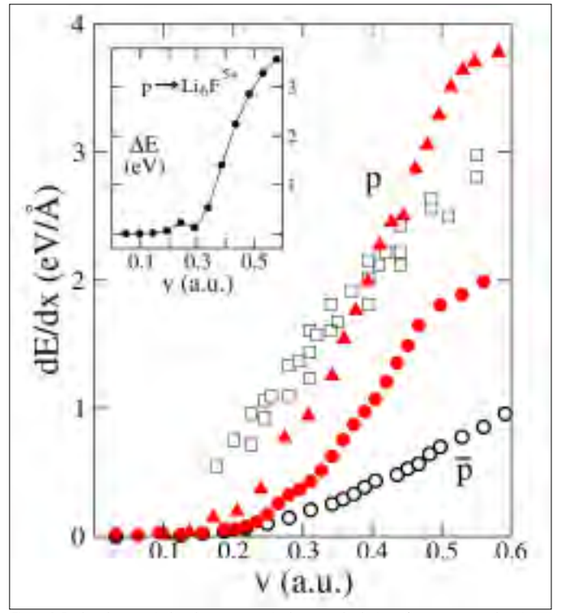

Figure 1: Red and open circles show, respectively, our calculations for protons and antiprotons using only the orbitals linked to the Li and F atoms as a basis set. Red triangles show the results using a more complete basis set that includes s and p orbitals linked to the protons. Open squares show the experimental results of references [2] and [3] for protons multiplied by a 1/2 factor to take into account the effects of channelling conditions, for which the calculations are performed. The inset shows the energy loss for protons colliding with a Li_6F^{5+} cluster. The similar behavior of the curves for the minimal cluster and the solid indicates the locality of the energy loss processes.

First-principles time-dependent quantum simulations are used, for the first time, to study the rate of energy transfer from a moving proton and antiproton to an insulator.

Following pioneering work for the stopping power of clusters of simple metals[1], the present work proposes a direct way of obtaining the needed information using time-dependent first-principles calculations. We have studied the case of protons shot through lithium fluoride, the best studied system in the field, obtaining promising agreements with what is experimentally known (like the ratio between the stopping powers of protons and antiprotons). Our results support the velocity threshold idea, including fair quantitative estimates. Some of them are shown in Figure 1. The study opens the field for analogous studies on materials of interest for nuclear engineering, waste containment, and biomedicine.

[1] M. Quijada, A.G. Borisov, I. Nagy, R. Díez-Muiño, and P.M. Echenique, Phys. Rev. A **75**, 042902 (2007).
[2] M. Draxler, S. P. Chenakin, S. N. Markin, and P. Bauer, Phys. Rev. Lett. **95**, 113201 (2005).
[3] S.P. Møller, A. Csete, T. Ichioka, H. Knudsen, U.I. Uggerhøj, and H.H. Andersen, Phys. Rev. Lett. **93**, 042502 (2004).

Modeling Nanostructures with Vicinal Surfaces

A. Mugarza[1], F. Schiller[1], M. Corso[1,2], J. Cordón[1], M. Ruiz-Osés[1], and J.E. Ortega[1,2]

Vicinal surfaces of the (111) plane of noble metals are characterized by free-electron-like surface states that scatter at one-dimensional step edges. We use STM and high-resolution, angle-resolved photoemission to thoroughly explore the geometry and the electronic surface states on a variety of vicinal surface structures. In regular step superlattices surface states smoothly switch from one-dimensional (1D) to two-dimensional (2D) by varying the lattice constant. Recently we have examined double-phase, faceted surfaces, where both 1D and 2D states coexist.

Vicinal metal surfaces are model systems to test electron scattering and tune electron bands in metallic superlattices. In particular, noble metal surfaces vicinal to the (111) plane, since they possess a free-electron-like surface state that is easily identified in scanning tunnelling microscopy/spectroscopy (STM/STS) and well characterized in angular photoemission (ARPES). In the past few years, our laboratory has devoted a considerable effort to the study of the electronic structure of noble metal vicinal surfaces. In general we observe important variations in surface state properties as the surface structure changes. Moreover, a clear understanding of surface states in vicinal metal surfaces requires a real space description of the wave fucntions, which is achieved by analyizing the three-dimensional (k_x, k_y, k_z) Fourier space of the electron with ARPES[1].

In simple 1D step arrays, the most remarkable property of surface states is their changing dimensionality, which varies from 1D to 2D as the lattice constant d, namely the terrace width is reduced. This reflects the fact that the repulsive barrier strength at step edges decreases by an order of magnitude from a surface with relatively wide d › 5 nm terraces to surfaces with smaller d ‹ 2nm lattice constant. The change in dimensionality of surface states is accompanied by a tilt in the modulation plane of the wave function from terrace-like in 1D states to average-surface-like in 2D bands. Such exotic behavior of surface states in step lattices can be explained by the progressive reduction of the bulk band gap projected on the surface plane[1].

A clear understanding of surface states in vicinal metal surfaces requires a real space description of the wave functions, which is achieved by analyizing the three-dimensional (k_x, k_y, k_z) Fourier space of the electron.

1 Departamento de Física Aplicada I and Centro de Física de Materiales-CSIC, UPV/EHU, San Sebastián, Spain **2** Donostia International Physics Center, San Sebastián, Spain

Published in **JPhys**

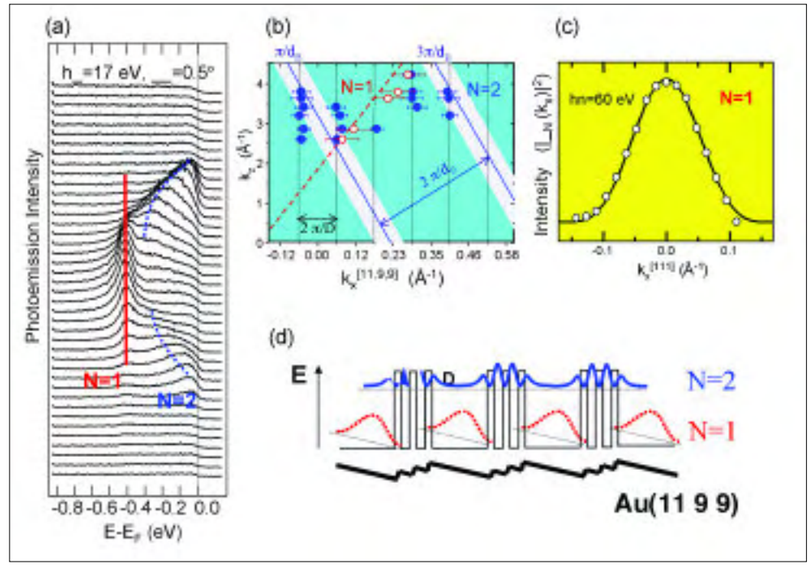

Periodic faceting of Au(111) leads to split-off surface states, namely a one-dimensional, lower energy state confined in terraces plus a two-dimensional, higher energy band, extended over the whole surface, but modulated by step bunches.

Following the same analytical framework developed for 1D step arrays, in this work we have analyzed surface states of complex, faceted Au(111) surfaces. In particular the Au(11,9,9) plane, which is a periodically faceted surface made of wide d_A=4.2 nm terraces and 2-3 step bunches (d_B=1.4 nm wide), as schematically depicted in the figure, panel (a). We present the high-resolution ARPES measurements. By selecting an appropriate photon energy (17 eV) one is able of separating a sharp, non-dispersing *N=1* level from a broad, dispersing *N=2* band. In order to unveil the physical nature of both states, we examine the (k_x,k_z) plot in panel (b), and analyze the k_x-dependent photoemission intensity in panel (c). This is needed to obtain the qualitative description of the electron wave functions for *N=1* and *N=2* states shown in (d). The *N=1* peak leads to a single set of data points along the [111] direction in the (k_x,k_z) plot, and to a probability density $|Y(k_x)|^2$ that fits to that of the *N=1* state of an infinite QW of size d_A. Such behavior is indeed expected for a 1D QW mostly located inside terraces, as indicated in panel (d). On the other hand, the photon-energy analysis of the dispersing *N=2* band leads to five sets of vertical $2\pi/D$ umklapps ($D=d_A+2d_B$) in the (k_x,k_z) plot of panel (b), with the photoemission intensity peaking at data sets separated by $2\pi/d_B$. These are indeed the features for a 2D surface state strongly modulated within the step bunch, but propagating on the surface plane along the k_x direction, as shown in panel (d).

In summary, periodic faceting of Au(111) leads to split-off surface states, namely a 1D lower energy state confined in terraces plus a 2D, higher energy band, extended over the whole surface, but modulated by step bunches.

[1] "Electronic States at Vicinal Surfaces", A. Mugarza and J.E. Ortega, J. Phys.: Condens. Matter **15**, S3281 (2003).

Unconventional Scenarios for Dynamic Arrest in Binary Mixtures

A.J. Moreno[1,2] and J. Colmenero[1,2,3]

We investigate slow dynamics in glass-forming binary mixtures with large dynamic asymmetry. Novel relaxation features are observed for both components, as logarithmic decays for density correlators. These features are assigned to an inherent higher-order point within the framework of the Mode Coupling Theory (MCT) of the glass transition. The former would originate from the coexistence of two different mechanisms for dynamic arrest. In the case of the fast component (small particles) such mechanisms would be packing induced by the neighboring fast particles, and confinement induced by the slow host matrix (large particles). In the case of the slow component they would be packing induced by the neighboring large particles, and depletion-mediated attraction induced by the small particles.

The rheological properties of soft-matter-based systems can be manipulated by a proper addition of components of very different mobilities. A large time scale separation between the two components in the mixture can be achieved for components with very different molecular size if the concentration of the small (fast) component is low or moderate.

In this work we perform the first investigation on slow structural relaxation in binary mixtures over the whole range of composition and size ratio. We carry out molecular dynamics simulations in a simple soft-sphere mixture. We find that these types of binary mixtures exhibit unusual relaxation features that challenge standard pictures for dynamic arrest in glass-forming systems. In the usual scenario, mean-squared displacements and density correlators display, respectively, a two-step increase and decay. The plateau arising at intermediate times between the microscopic and diffusive regimes characterizes the caging regime, i.e., the temporary trapping of each particle by its neighbors. Binary mixtures with strong dynamic asymmetry do not exhibit, for selected values of the control parameters, a defined plateau. The decay of density correlators can be purely logarithmic over several time decades.

Simulation data have been analyzed in the framework of the Mode Coupling Theory (MCT) of the glass transition. This theory predicts a transition from an ergodic to a non-ergodic ('glassy') state at a critical temperature T_c. The latter is manifested in density correlators by a jump of their long-time limit (non-ergodicity parameter) from zero to a finite value. If the latter performs a finite jump the transition is denoted as 'type-B'. If it increases continuously from zero it is denoted as 'type-A'. For temperatures close to T_c, MCT predicts several scaling laws for density correlators. The associated dynamic exponents are univocally related to a single one ($\lambda \leq 1$). The latter parameter is also univocally determined by static correlations at the critical temperature. A detailed test of scaling predictions of MCT

1 Instituto de Ciencia de Materiales de Barcelona-CSIC), Bellaterra, Spain **2** Department of Physics, University of California, Berkeley, California, USA **3** Donostia International Physics Center, San Sebastián, Spain **4** Centro de Física de Materiales-CSIC, UPV/EHU, San Sebastián, Spain **5** Departamento de Física de Materiales, Facultad de Química, San Sebastián, Spain **6** Department of Earth Sciences, University of Cambridge, UK

Published in **JPhys**

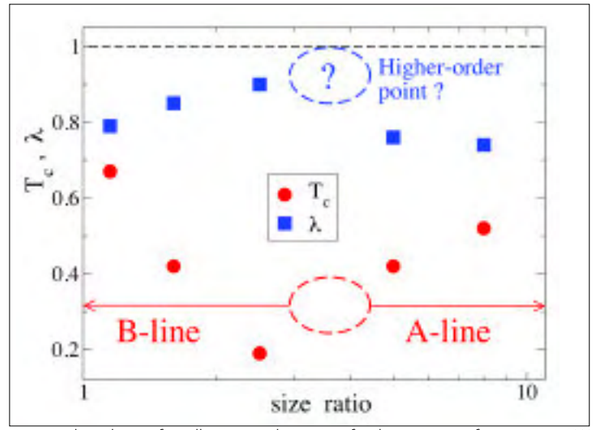

Dynamic phase diagram for collective correlations in soft-sphere mixtures of composition 40% large-60% small.

Anomalous relaxation originates from the coexistence of two mechanisms for dynamic arrest.

is performed as a function of the size ratio. The Figure displays the so-obtained dynamic phase diagram for collective correlations in soft-sphere mixtures. Re-entrant behavior is observed for the critical temperature and the λ-parameter. For a size ratio of about 3 the value of λ approaches unity and collective density correlators exhibit logarithmic decays. In the framework of MCT both features are connected to an underlying higher-order critical point ($\lambda \rightarrow 1$). This type of transition and the associated anomalous relaxation originates from the coexistence of two mechanisms for dynamic arrest, with different characteristic lengths. In the case of the small particles such mechanisms would be packing induced by the neighboring small particles, and confinement induced by the slow matrix formed by the large particles. In the case of the large particles they would be packing induced by the neighboring large particles, and depletion-mediated attraction induced by the small particles.

Also in agreement with MCT, self- and collective correlations for the small particles exhibit, for very large size ratio, different temperatures for dynamic arrest. Self-correlations remain ergodic below the critical temperature for collective correlations, which freeze together with self- and collective correlations of the large particles. Freezing of collective correlations for the small particles occurs over a type-A line, differently from the standard B-line observed at smaller size ratio for the small particles, and at all size ratios for the large particles. The A- and B-lines seem to merge in the higher-order point. This full dynamic decoupling between self- and collective dynamics of the small particles can be understood as follows. The large particles form a stable glassy matrix that only exhibits residual vibrations. The small particles can diffuse over the network of interconnected voids inherent to the host matrix. This network is permanent, leading to frozen collective correlations of the small particles, but diffusion yields full relaxation of self-correlations.

The unified picture presented in this work shares features with partial observations in glass-forming mixtures of very different nature as polymer blends, colloidal mixtures, star polymer solutions, or ion conducting glasses, and suggests a common MCT scenario for this large family of systems.

A.J. Moreno and J. Colmenero, J. Chem. Phys. **124**, 184906 (2006); Phys. Rev. E **74**, 021409 (2006); J. Chem. Phys. **125**, 164507 (2006); J. Phys.: Condens. Matter **19**, 466112 (2007).

Slow Dynamics in a Novel State of Soft Matter

A.J. Moreno[1,2,3] and C.N. Likos[3]

For a large class of fluids interacting via ultrasoft bounded potentials, particles form crystals consisting of clusters located in the lattice sites, with a density-independent lattice constant. Here we present an investigation on the dynamic features of a representative example of this class of fluids. It is found that particles diffuse between lattice sites, through an activated hopping mechanism. Though, by means of this mechanism, clusters fully change their initial identity, the crystal lattice is stable. Hopping leads to finite values for the diffusivity and full relaxation of density correlation functions. Simulations suggest the existence of a localization transition which is avoided by hopping events, and dynamic decoupling between self- and collective correlations.

The investigation of large-scale structural and dynamic properties of macromolecular solutions can be facilitated by coarse-graining the intramolecular fast degrees of freedom. By following this procedure, each macromolecule is represented as a single particle interacting with any other through an effective ultrasoft pair potential, which for isotropic interactions just depends on the distance between centers-of-mass. The effective potential is bounded if centers-of-mass can coincide without violating excluded volume conditions. Some examples are polymer chains, dendrimers or microgels, in dilute or semiconcentrated solution.

Generalized exponential models (GEM), $V(r) = \varepsilon\exp[-(r/\sigma)^n]$, where σ is of the order of the macromolecule size, constitute a class of such effective bounded interactions. The cases $n \leq 2$ and $n > 2$ belong respectively to the so-called Q^+-and $Q^\pm$-classes for which the Fourier transform of $V(r)$ is, respectively, positive or oscillating around zero. According to a general criterion, based on a mean-field density functional theory, systems belonging to the Q^+-class display re-entrant crystallization in the density-temperature plane. Systems of the $Q^\pm$-class display a monotonic freezing line beyond which the system forms cluster crystals. Clustering is encountered even if the effective interaction is *purely repulsive*, as in the present case. These are novel forms for the self-organization of soft matter, since they feature a lattice constant that is density-independent. In other words, the cluster population is proportional to the density. It must be stressed that the investigation of the structural and dynamic properties of this class of fluids is not a merely academic question. Recent simulations of amphiphilic dendrimers show that the latter indeed interact via an effective GEM-potential of the $Q^\pm$-class!

In this work we have carried out molecular dynamics simulations for a system of particles interacting via a GEM-potential with $n = 8$. We have investigated slow dynamic features in the cluster crystal phase. Figure 1 shows a typical configuration of the system beyond the freezing point. Particles form

1 Donostia International Physics Center, San Sebastián, Spain **2** Centro de Física de Materiales-CSIC, UPV/EHU, San Sebastián, Spain **3** Institut für Theoretische Physik II, Heinrich-Heine-Universität Düsseldorf, Germany

Published in **PRL**

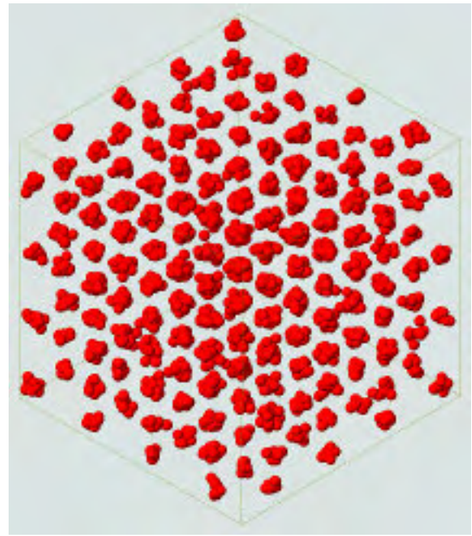

Figure 1: A typical configuration of the system at number density $\rho = 7s\sigma^{-3}$.

Particles form cluster crystals. These are novel forms for the self-organization of soft matter, since they feature a lattice constant that is density-independent.

clusters located at the sites of a fcc lattice. The latter structure is the stable state according to free energy calculations, and indeed is not distorted within the simulation time window.

Figure 2 displays the typical behavior, in the fcc phase, of the van Hove self-correlation function (i.e., the histogram of particle displacements) at different times. The latter broadens with time, developing maxima and minima centered around lattice distances. At the limit of the simulation window, more than 70 % of the particles have moved beyond their initial lattice site. Therefore, particles perform hopping motion between neighbouring clusters, which fully changes their initial identity, but does not destroy the lattice structure. The measured diffusivity is indeed finite and follows Arrhenius behavior, with an activation energy proportional to the mean cluster population (i.e., to the density). The presence of a marked minimum at $r/d_{nn}=2^{1/2}$ and a sharp maximum at $r/d_{nn}=3^{1/2}$ suggest a preferential directionality for the motion between neighboring sites, with low and high probability for angles of, respectively 90° and 120° between consecutive jumps.

We have also computed self- and collective (pair) density correlation functions. An unusual decoupling between self- and collective dynamics is observed. In analogy with plastic crystals, the localization transition for pair correlations not probing the reciprocal lattice occurs at a lower temperature than that for self-correlations. However, the mentioned hopping events restore ergodicity at long times, leading to full relaxation of both self- and collective correlations.

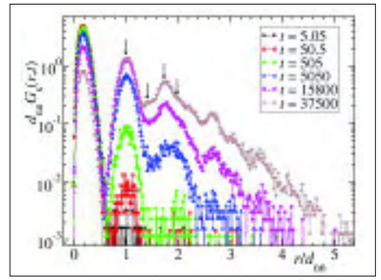

Figure 2: Van Hove self-correlation function for different times (in units of $\sigma[m/\varepsilon]^{1/2}$), at number density $\rho = 2s\sigma^{-3}$ and temperature T = 0.267ε. Displacement is scaled by the distance between nearest-neighbor lattice sites, d_{nn}. Arrows indicate fcc lattice sites.

A.J. Moreno and C.N. Likos, Physical Review Letters **99**, 107801 (2007).

Published in **PRL**

Dimensionality Effects in the Optics of Boron Nitride Nanostructures: Applications for Optoelectronic Devices

L. Wirtz[2], C. Attacalite[1], A. Marini[3], and A. Rubio[1]

We illustrate the effect of dimensionality and electron-hole attraction in boron nitride (BN) compounds. The optical absorption spectra of BN nanotubes are dominated by strongly bound excitons. The absolute position of the first excitonic peak is almost independent of the tube radius and system dimensionality. This provides an explanation for the observed "optical gap" constancy for different tubes and bulk hexagonal BN. Furthermore, the levels which are responsible for defect-mediated photo-luminescence are shifted by the electric field making BN nanotubes excellent candidates for optoelectronic applications in the UV and below.

Boron nitride is currently used as a coating material for reactors and as an insulating material. However, its intriguing electronic properties, which include high resistance, and blue light emission make it a potentially useful material for the development of optoelectronics in optical data storage media and as high resolution UV lasers as well as in telecommunications. Boron nitride is isoelectronic with carbon and so can exist in isomorphic forms equivalent to diamond, graphite, and even the spherical fullerenes and the cylindrical tubes. Specifically, hexagonal boron nitride is analogous to graphite, but whereas graphite is electrically conductive, hexagonal BN is an insulator.

The optical properties of BN nanotubes are quite unusual and cannot be explained by conventional theories. Because of the reduced dimensionality of the nanotubes, both quasiparticle and excitonic many-electron effects are extraordinarily important in carbon nanotubes[1] and BN nanotubes[2]. A striking effect is observed in the Figure: the electron-hole attraction modifies strongly the independent particle spectra (RPA) concentrating most of the oscillator strength in one active excitonic peak. The position of this peak is rather insensitive to the dimensionality of the system, in contrast to the RPA calculation (not shown), where the shape of the spectra of the nanotubes depends strongly on the nanotube diameter. The main effect of the dimensionality appears in the onset of the continuum excitations and in the set of excitonic series above the main active peak. In spite of the fact that the binding energy for the first and dominant excitonic peak depends sensitively on the dimensionality of the system, varying from 0.7 eV in bulk BN to 3 eV in the hypothetical (2, 2) tube, the position of the first optically active excitonic peak is almost independent of the tube radius and system dimensionality. The reason for this subtle cancellation of dimensionality effects in the optical absorption stems from the strongly localized nature of the exciton (see Figure). Experimental data and calculations show an outstanding agreement, not only on the constancy of the band gap but on the whole spectral function. We remark that dimensionality effects would be more noticeable in other spectroscopic measurements, such as photoemission spectroscopy, where one mainly maps the quasiparticle spectrum. In particular the quasi-particle band-gap will vary strongly with dimensionality, opening up as the dimensionality is reduced. The situation is different in carbon nanotubes, where excitonic effects are also very important but they depend on the specific nature of the tube.

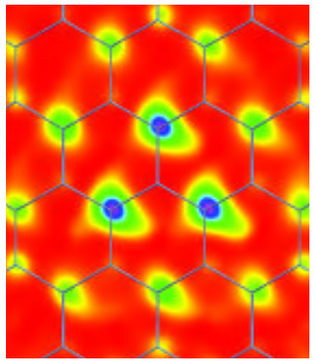

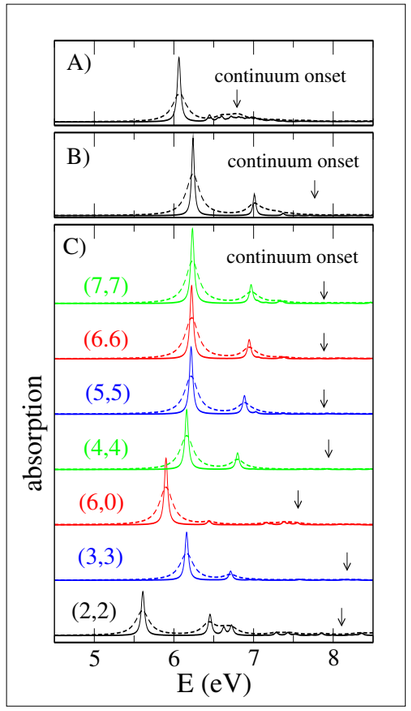

Simulations indicate new ways to exploit the electronic and mechanical properties of hexagonal boron nitride.

Even though the bandgap of the tubes decreases strongly as a function of the electric field strength, the absorption spectrum remains remarkably constant up to high field-strength. However, we have recently found[3] that defect-levels within the gap are shifted by the electric field. This may have a strong impact on defect-mediated photo-luminescence and opens up the road for the use of BN nanotubes as optoelectronic devices (emission tuneable from the UV to the visible regime with high yield).

[1] C.D. Spataru, S. Ismail-Beigi, L.X. Benedict, and S.G. Louie, Phys. Rev. Lett. **92**, 077402 (2004).
[2] L. Wirtz, A. Marini, and A. Rubio, Phys. Rev. Lett. **96**, 126104 (2006).
[3] C. Attacalite, L. Wirtz, A. Marini, and A. Rubio, Phys. Stat. Sold. (b) **244**, 4288 (2007).

1 Donostia International Physics Center, Centro de Física de Materiales-CSIC, UPV/EHU and European Spectroscopy Facility-UPV/EHU, San Sebastián, Spain **2** Institute for Electronics, Microelectronics, and Nanotechnology (IEMN), Villeneuve d'Ascq, France **3** Instituto Nazionale per la Fisica della Materia and Dipartimento di Fisica, Università di Roma, Italy

Metal-Organic Honeycomb Nanomeshes with Tunable Cavity Size

U. Schlickum[1], R. Decker[1], F. Klappenberger[1,6], G. Zoppellaro[2], S. Klyatskaya[2], M. Ruben[1,2], I. Silanes[3], A. Arnau[3], K. Kern[1,4], H. Brune[1], and J.V. Barth[1,5,6]

We present a systematic study of metal-organic honeycomb lattices assembled from simple ditopic molecular bricks and Co atoms on Ag(111). This approach enables us to fabricate size- and shape-controlled open nanomeshes with pore dimensions up to 5.7 nm. The networks are thermally robust while extending over μm^2 large areas as single domains. They are shape resistant in the presence of further deposited materials and represent templates to organize guest species and realize molecular rotary systems.

Supramolecular chemistry with its unique control of highly organized molecular architecture and intrinsic defect correction is an efficient synthetic tool for nanoscale control of matter. In particular, the development of metallosupramolecular self-assembly techniques gives access to a variety of grid structures based on the coordination of organic linkers with metal centers.[1-3] Recent studies revealed that low dimensional coordination networks bearing potential for technological applications can be similarly realized on well defined surfaces.[4-6] Notably rectangular networks could be realized on square substrates featuring open cavities in the 0.5-2 nm range.[5] Here, we report on a methodology to design highly regular size- and shape-controlled nanomeshes with tunable pore size, based on the transition metal-directed assembly of ditopic organic linkers on a Ag(111) substrate. The underlying threefold Co-carbonitrile coordination motif is examined with the help of first-principles calculations. By varying the length of the custom-designed polyphenyldicarbonitrile linkers, we realized open honeycomb networks comprising hexagonal pores up to 5.7 nm in diameter. The pertaining shape-resistant nanocavities provide an ideal playground for many further studies. In particular, we demonstrate their capability to spatially confine guest species and observe their restricted lateral motion.

The objective of our investigation is the development of a rationale for surface-confined supramolecular chemistry, which will offer an exquisite tool for the massively parallel construction of extended, defect-free regular two-dimensional(2D) nanoporous networks. We devised a series of simple ditopic dicarbonitrile polyphenyl molecular linkers (abbreviated NC-Phn-CN, whereby n can be 3, 4, or 5; see Figure 1). All ditopic molecular bricks have the same functional carbonitrile endgroups, while their lengths increase with n from 1.66 via 2.09 up to 2.53 nm. In all cases, highly regular arrays comprising nanometer-sized honeycomb cavities are formed. In addition, the cavity size is shown to be tunable and nearly triples the fabricated maximum mesh size with the NCPh5-CN linkers.

A methodology to design nanomeshes with tunable pore size.

1 Institut de Physique des Nanostructures, École Polytechnique Fédérale de Lausanne, Switzerland **2** Institut für Nanotechnologie, Forschungszentrum Karlsruhe, Germany **3** Donostia International Physics Center and Departamento de Fisica de Materiales and Unidad de Fisica de Materiales, San Sebastian, Spain **4** Max-Planck-Institut für Festkörperforschung, Stuttgart, Germany **5** PHAS-AMPEL, University of British Columbia, Vancouver, Canada **6** Physik Department E20, Technische Universität München, Garching, Germany

Published in **NANOLett**

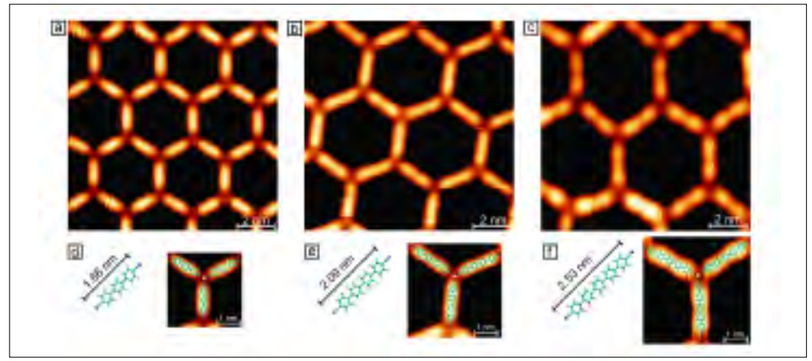

Figure 1: Tuning the cavity size of metal-organic honeycomb networks with designed linkers. The STM images show the result of Co-directed assembly of (a) NC-Ph3-CN, (b) NC-Ph4-CN, and (c) NC-Ph5-CN, respectively. (d-f) Structure of the molecules including their length and models of the threefold Co-carbonitrile coordination motif resolved in (a-c) (yellow, cobalt center; turquoise, carbon; white, hydrogen; blue, nitrogen). The images (a-c) were taken at a tunnel current of *I*) 0.1 nA and bias voltages of 0.9, 1, and 2 V, respectively.

DFT calculations help to uncover the origin of threefold coordinated Co centers.

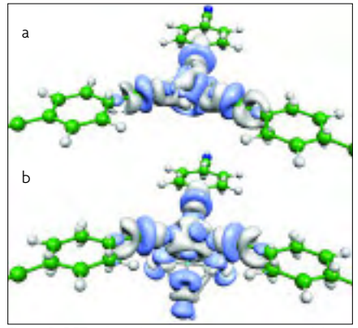

Figure 2: DFT calculations help to uncover the origin of threefold coordinated Co centers. (a,b) Plots of the induced charge density around the cobalt atom in threefold coordination of a model compound (NC-Ph1-CN) without (a) and with (b) the presence of an Ag_4 cluster underneath the transition metal center. The image displays the electron density redistribution around the Co atom due to the bond formation with the ligands and the Ag_4 cluster. Light blue color means charge depletion, and light gray charge accumulation (0.002 e/Å^3).

Density functional theory (DFT) calculations[7] indicate that the encountered threefold coordination motif, uncommon for bulk transition metal-carbonitrile complexes is induced by the presence of a metal substrate. To assess the interaction of the Co center with the underlying surface, we performed calculations of both free planar compounds and complexes where a cluster of four Ag atoms was placed underneath the coordinated Co atom (see Figure 2). The comparison between threefold and fourfold coordination was made by calculating the total binding energy of the complete system. The consideration of the binding energies within the node indicates that the interaction of the cobalt atoms with the surface is a key factor in favoring a 2D network with a threefold coordination of the organic ligands.

The metal-organic networks themselves provide a basis for a variety of further experiments because they are stable at temperatures up to 300 K and shape-persistent in the presence of additionally deposited materials, even for transition metal atoms (Fe). Thus, the honeycomb networks can serve as templates to organize coadsorbed molecular species and to study molecular motion processes in confined environments. The achieved molecular organization and the tip-induced motions within the cavities reveal that networks qualify for spatial confinement of guest species.

[1] B.J. Holiday, C.A. Mirkin, Angew. Chem., Int. Ed. **40**, 2022-2043 (2002).
[2] O.M. Yaghi, M. O'Keeffe, N.W. Ockwig, H.K. Chae, M. Eddaoudi, J. Kim, Nature **423** (6941), 705-714 (2003).
[3] M. Ruben, J. Rojo, F.J. Romero-Salguero, L.H. Uppadine, J.-M. Lehn, Angew. Chem., Int. Ed. **43**, 3644-3662 (2004).
[4] A. Dmitriev, H. Spillmann, N. Lin, J.V. Barth, K. Kern, Angew. Chem., Int. Ed. **41**, 2670-2673 (2003).
[5] S. Stepanow, M. Lingenfelder, A. Dmitriev, H. Spillmann, E. Delvigne, N. Lin, X. Deng, C. Cai, J.V. Barth, K. Kern, Nature Mat. **3**, 229-233 (2004).
[6] J.V. Barth, G. Costantini, K. Kern, Nature **437**, 671-679 (2005).
[7] J.M. Soler, E. Artacho, J.D .Gale, A. Garcia, J. Junquera, P. Ordejón, D. Sanchez-Portal, J. Phys. C: Cond. Matt. **14**, 2745-2780. (2002).

Structures and Potential Superconductivity in SiH_4 at High Pressure— En Route to "Metallic Hydrogen"

J. Feng[1], W. Grochala[1,2], T. Jaroń[3], R. Hoffmann[1,2], A. Bergara[4] and N.W. Ashcroft[2,5]

Recently reported superconductivity in lithium under pressure has renewed the interest on hydrogen and hydrogen-rich systems in the long standing conquest of room temperature superconductivity. In this article we have presented an *ab initio* analysis of pressure induced metallization of silane. The most stable structure found can be metallized at an experimentally accessible pressure of around 90 GPa and, according to a BCS-like estimate, metallic silane could also be a high temperature superconductor.

Metallization of solid hydrogen under pressure is one of the still unsolved interesting topics in Condensed Matter Physics, and recent experiments indicate that the expected metallic transition (at around 450 GPa, about 4.5 million atmospheres) cannot be reached yet within current experimental capabilities[1]. A great expectation exists around the metallic transition in hydrogen, because, among other things, metallic hydrogen might be a superconductor with a very high Tc[2], which basically relays on its high Debye temperature associated to the light mass of hydrogen, that could be also extended to other light metals and its alloys.

Although recent experiments looking for superconductivity at ambient pressure in the next lightest alkali (lithium) have shown to be as low as 0.4 mK[3], lithium under present presents a unexpected strong modification of its bonding and electronic properties under pressure[4]. Even more interestingly, it has shown to superconduct at around 20 K when the applied pressure rises to 30 GPa[5], becoming one of the elements with the highest superconducting transition temperature. These observations have recently raised the interest on metallic hydrogen and hydrogen-rich alloys (e.g., group IV hydrides)[6]. One can view the hydrogen in these systems as being *chemically precompressed* by a heavier element and a lower external pressure might be required to get its metallization. In this work we have examined this possibility in detail, along the way predicting the metallization pressure of SiH_4 (since CH_4 has shown to remain insulating up to 500 GPa[7]) and estimating the key quantities associated with its critical superconducting temperature.

One can view the hydrogen as being *chemically precompressed* by a heavier element and a lower external pressure might be required to get its metallization.

1 Department of Chemistry and Chemical Biology, Cornell University, New York, USA **2** Cornell Center for Materials Research, Cornell University, New York, USA **3** Department of Chemistry, University of Warsaw, Poland **4** Materia Kondentsatuaren Fisika Saila, UPV/EHU and Donostia International Physics Center, San Sebastián, Spain **5** Laboratory of Atomic and Solid State Physics and Department of Physics, Cornell University, New York, USA

Published in **PRL**

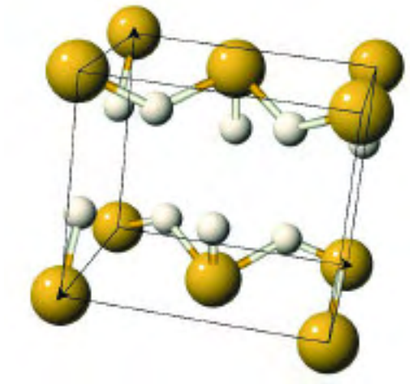

Since the crystal structure of solid silane is not known at high pressures[8], in order to survey a range of possible coordination and paking modes, in our theoretical *ab initio* study we have considered a total of 13 quite different structures. Our calculations indicate that with increasing pressure, covalent-like structures with a higher coordination number begin to be preferred over the molecular solid, and above 27 GPa the most stable one becomes the layered *Pmna* structure (figure), which can be described as sheets of octahedrally coordinated Si atoms (yellow) sandwiched between layers formed by H (white) double sheets. As expected, on compression the band gaps decrease and the preferred *Pmna* structure metallizes when r_s=0.88 A (at 91 GPa), in agreement with the general Goldhammer-Herzfeld criterion.

General main arguments favoring the enhanced superconducting transition temperature in hydrogen can be also applied to these compounds[6], and in order to derive a first estimate of Tc we have simply used a BCS approach. The quasi-2D appearance of the metallic form of *Pmna* SiH4 suggests that the motion of terminal H atoms parallel to the puckered SiH2 plane should have the greatest influence on pairing of mobile charge carriers. Examining the phonons at the onset of metallization, shows that its Debye temperature (3500 K) is superior by 2 orders of magnitude to that for Pb, (a classical strong-coupling superconductor with a Tc of 7.2 K), and makes silane to be a potential candidate for a high-Tc superconductivity.

These results have motivated the interest of several experimental groups and, interestingly, our predicted metallization of silane has been confirmed by very recent optical experiments[9], where a Drude-like behavior has been observed above 60 GPa. Additionally, main physical features presented here are not unique of compressed silane, but have been also predicted to occur in other heavier hydrides (e.g., GeH_4[10] and SnH_4[11]).

[1] P. Loubeyre, F. Occelli, and R. LeToullec, Nature, **416**, 613 (2002).
[2] N.W. Ashcroft, Phys. Rev. Lett. **21**, 1748 (1968).
[3] J. Tuoriniemi, K. Juntunen-Nurmilaukas, J. Uusvuori, E. Pentti, A. Salmela and A. Sebedash, Nature **447**, 187 (2007).
[4] V.M. Silkin, A. Rodriguez-Prieto, A. Bergara, E. V. Chulkov, and P. M. Echenique, Phys. Rev. B **75**, 172102 (2007); A. Rodriguez-Prieto, A. Bergara, V. M. Silkin, and P. M. Echenique, Phys. Rev. B **74**, 172104 (2006); A. Rodriguez-Prieto and A. Bergara, Phys. Rev. B **72**, 125406 (2005); A. Bergara, J.B. Neaton, and N.W. Ashcroft, Phys. Rev. **B62**, 8494 (2000); M. Hanfland, K. Syanssen, N.E. Christensen, and D.L. Novikov, Nature **400**, 174 (2000); J.B. Neaton and N. W. Ashcroft, Nature **400**, 141 (1999).
[5] V.V. Struzhkin, M.I. Eremets, W. Gan, H. Mao, R.J. Hemley, Science **298**, 1213 (2002); K. Shimizu, H. Ishikawa, D. Takao, T. Yagi, and K. Amaya, Nature **419**, 597 (2002); N.W. Ashcroft, Nature **419**, 569 (2002); S. Deemyad and J. S. Schilling, Phys. Rev. Lett. **91**, 167001 (2003).
[6] N.W. Ashcroft, Phys. Rev. Lett. **92**, 187002 (2004).
[7] M. Martinez-Canales and A. Bergara, High Press. Res. **26**, 369 (2006).
[8] Olga Degtyareva, Miguel Martínez Canales, Aitor Bergara, Xiao-Jia Chen, Yang Song, Viktor V. Struzhkin, Ho-kwang Mao, and Russell J. Hemley, , Phys. Rev. B **76**, 064123 (2007).
[9] Xiao-Jia Chen, Viktor V. Struzhkin, Yang Song, Alexander F. Goncharov, Muhtar Ahart, Zhenxian Liu, Ho-kwang Mao, and Russell J. Hemley, PNAS **105**, 20 (2008).
[10] M. Martinez-Canales, A. Bergara, J. Feng, and W. Grochala, J. Phys. Chem. **67**, 2095 (2006).
[11] Y. Yao, J. S. Tse, Y. Ma and K. Tanaka, Europhysics Letters **78**, 37003 (2007).